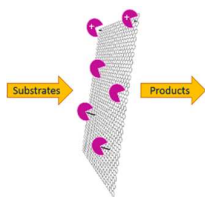




Controlling enzyme function through immobilisation on graphene, graphene derivatives and other two dimensional nanomaterials

Journal:	<i>Journal of Materials Chemistry B</i>
Manuscript ID	TB-REV-02-2018-000313.R1
Article Type:	Review Article
Date Submitted by the Author:	05-Apr-2018
Complete List of Authors:	Ramakrishna, Tejaswini; Deakin University School of Life and Environmental Sciences Nalder, Tim; Deakin University, Deakin University, Centre for Chemistry and Biotechnology, School of Life and Environmental Sciences Yang, Wenrong; Deakin University, ; The University of Sydney, Marshall, Sue; Plant and Food research, Natural extracts Barrow, Colin; Deakin University, Bio-Deakin

A table of contents entry



Controlling enzyme function through immobilisation on graphene, graphene derivatives and other two dimensional nanomaterials.



Journal Name

ARTICLE

Controlling enzyme function through immobilisation on graphene, graphene derivatives and other two dimensional nanomaterials

Tejaswini Rama Bangalore Ramakrishna,^{a,b} Tim D. Nalder,^{a,b} Wenrong Yang,^{a*} Susan N. Marshall^b and Colin J. Barrow^a

Received 00th January 20xx,
Accepted 00th January 20xx

DOI: 10.1039/x0xx00000x

www.rsc.org/

Robust enzyme immobilisation methods that preserve enzyme activity while enabling enzymes to be recovered and reused multiple times have important applications in biocatalysis. However, immobilisation can change the functionality of enzymes, both in terms of their level of activity and their selectivity. These changes in activity are unpredictable and at present cannot be controlled, but if fully understood at a fundamental level could offer the opportunity to create highly targeted enzyme systems for specific applications. In this review, we will highlight the use of two dimensional nanomaterials (2D NMs), particularly graphene and its derivatives, as immobilisation materials to modify and control the selectivity and activity of various enzymes. The fundamental information obtained from immobilising enzymes on 2D NMs allows for the implementation of improved immobilisation strategies and assists in the design of next generation nano- and macro-materials for enzyme immobilisation. We hope that this review will highlight the potential for tailoring enzyme activity and selectivity through immobilisation.

1. Introduction

Graphene, the world's first two dimensional nanomaterial (2D NM), was isolated by Andre Geim and Konstantin Novoselov in 2004.¹ They used a simple scotch tape method to peel off single layers of graphene from graphite flakes. The material was found to be atomically flat and possessed useful properties, such as high surface area,^{2,3} optical transparency,^{4,5} flexibility⁶ and mechanical strength,⁷ as well as electronic and thermal conductivity.^{8,9} The combination of these exceptional qualities has attracted interest in the use of 2D graphene in the development of energy storage devices¹⁰⁻¹² and in bio-applications.¹³⁻¹⁵ Following the discovery and characterisation of graphene, the demand for the development of other 2D NMs has grown significantly. Examples of 2D NMs that followed graphene include graphene oxide (GO), boron nitride (BN), synthetic silicate clays, layered double hydroxides (LDHs), transition metal dichalcogenides (TMDs) and transition metal oxides (TMOs).¹⁶⁻¹⁸ Over the past decade research into the utilisation of 2D NMs has increased significantly, including recent use of graphene and graphene oxides as enzyme immobilisation matrices/supports. The use of these 2D NMs represents an emerging field of research with exciting possibilities for providing both a fundamental understanding of immobilisation mechanisms and applied outcomes. 2D NMs possess many properties which make them well suited to enzyme immobilisation and the study thereof, including high surface area, dispersion in solution, tuneable surface

chemistries and the ability to retain water adlayers.

Enzymes are biocatalysts with utility in a wide range of applications, including use in the development of biosensors, food processing, detergents, textile processing, and the synthesis of pharmaceuticals and fine chemicals.¹⁹ The ability of different enzymes to function in a range of environments, from acting optimally under mild near-physiological conditions through to an ability to catalyse reactions at extreme temperature or pH, means that they can provide alternatives to conventional chemical and physical processing methods. The use of enzymes for specific applications provides benefits such as lower energy requirements, reduced chemical waste output, and greater reaction specificity and selectivity.²⁰ Industrially useful enzymes are generally immobilised on solid supports, allowing the enzymes to be reused in multiple reaction cycles and recovered from the reaction products so they do not remain as contaminants.²¹⁻²³ Immobilisation can improve enzyme stability and has the potential to modify the activity of bound enzymes with respect to specificity, regio-, chemo- and enantio-selectivity of enzymes.²⁴ In addition to the effect of the reaction conditions, the properties of immobilised enzymes are heavily dependent on the properties of the carrier material that is used for immobilisation. Furthermore, the approach used to bind the enzyme to the support surface will affect the resulting enzyme-support complex.

Retention of enzyme structure and activity, while interfacing enzymes with solid materials requires an understanding of the material architecture at the nanoscale. Graphene's properties, in particular its 2D form, allow for application of a number of analytical techniques in studying its surface and the molecules that are bound to it. Therefore interactions between enzymes and the surfaces they are bound to can now be studied at a single molecule

^a School of Life and Environmental Sciences, Deakin University, 75 Pigdons Road, Waurn Ponds, Victoria, Australia.

^b Seafood Unit, The New Zealand Institute for Plant & Food Research Limited, 293-297 Akersten Street, Nelson 7010, New Zealand

*Corresponding author: W.Y. wenrong.yang@deakin.edu.au

level, not previously possible with macro-materials. Graphene derivatives are attractive because of their easy synthesis at laboratory-scale and tuneable surface chemistry.^{16, 25, 26} Currently graphene-based materials cannot be produced in large enough quantities for the immobilisation of industrial biocatalysts, but they are useful tools for the study of immobilisation mechanisms at a fundamental level. In the future as new techniques are developed for the controlled production of graphene, these materials may provide attractive alternatives to traditional supports for industrial use. For now, graphene and other 2D NMs allow us to obtain fundamental mechanistic information that can inform the design of next generation nano- and macro-materials for use in enzyme immobilisation at both research and industrial scales. Where 2D NMs do currently have direct commercial applications is in the fabrication of biosensors, however with the exception of examples that have modified enzyme function, this topic will not be covered by this review.

Previous articles have reviewed the literature regarding the use of graphene and other 2D NMs and their use in a broad sense. The very first review discussing the interaction of graphene and graphene oxide with proteins and peptides was by Zhang et al.²⁷ Following this, enzyme immobilisation on a range of nanomaterials was reviewed with respect to application in biofuel cells.²⁸ More recently a number of review articles have covered the interaction and integration of biomolecules, including viruses, DNA, proteins, peptides and carbohydrates, with graphene nanocomposites, graphene and graphene derivatives.^{13, 29-32} However, there are no reviews that have systematically investigated the literature with regard to controlling enzyme function on 2D NMs. Herein we have reviewed the literature from the last 5 years on the use of these materials for enzyme immobilisation, with a particular focus on understanding and controlling enzyme properties and function on 2D NMs.

2. Properties of graphene and other two dimensional nanomaterials

Graphene, graphene derivatives and other 2D NMs possess a number of properties, such as high surface area, magnetism and conductivity³³, which make them suitable for use in enzyme immobilisation studies. High surface area is important for any immobilisation support as it allows for improved enzyme loading capacity. Traditional materials achieve high surface areas by using micro beads with very high surface to volume ratios, or highly porous macro resins. The very high specific surface area of 2D NMs, for example graphene (experimentally calculated at 700–1100 m²/g)^{34, 35} and its derivatives means that 2D NMs could provide useful alternatives. To fully utilise the benefits of 2D NMs as an enzyme immobilisation support it is crucial that its surface properties and architecture are understood at the nano level. Further to this, understanding how different fabrication methodologies and modifications to the surface chemistry effect the materials are key to their use. The following sections briefly highlight some of the fabrication techniques used to synthesise graphene and other 2D NMs, as well as the properties that make them highly useful supports for investigating enzyme-support interactions.

2.1 Fabrication of graphene and 2D NMs

The method of synthesis for producing graphene and manipulation of the surface chemistry can be used to control the functionality of enzymes subsequently bound to the 2D surface. The most commonly used methods of synthesis are mechanical exfoliation, chemical vapour deposition (CVD), spin coating and liquid exfoliation. Detailed reviews of the above methodologies used to synthesise 2D NMs have been published previously by our group.^{36, 37} A brief overview of mechanical exfoliation, CVD and spin coating methods is described below. Mechanical exfoliation involves the extraction of the top layer of a 3D material by breaking weak inter-layer bonds such as π - π stacking. A well know example is Novoselvo et al using scotch tape to isolate monolayer graphene from graphite flakes.¹ This approach is now also widely used to generate other 2D NMs such as BN and TMDs (i.e. NbSe₂, Bi₂Sr₂CaCu₂O_x and MoS₂).³⁸ The method enables the isolation of 2D NMs in a highly pristine (minimal defects) and stable form, although this method is not scalable. CVD is an alternative approach to producing monolayer 2D NMs.³⁹ It involves the use of a scaffold on which the 2D NMs are grown. After synthesis the scaffold is separated from the 2D NM via evaporation at ~1100 °C. The surface of the scaffold needs to be very different from that of the 2D NM for separation to occur. For example, zinc-sulphide nanoribbons, ammonia-borane with copper foil and stainless steel are different scaffolds used for growing monolayer BN nanoribbons, hexagonal BN and graphene sheets, respectively.³⁹⁻⁴¹ The method has disadvantages, particularly the difficulty in separating the 2D NM from the scaffold, as well as the requirement for high temperatures and the use of explosive gases as carbon feedstocks. Spin coating is used to synthesise layers of 2D NMs from their respective precursors. For the production of graphene, polystyrene is used as a precursor, which is deposited onto a Ni substrate and heated in an argon atmosphere.⁴² For MoS₂, dimethylformamide is used as the precursor along with n-butyl amine and 2-aminethanol to produce wafer-scale MoS₂.⁴³ Even though the spin coating method is simple there are disadvantages in the requirement for high temperatures (~800–1000 °C) to produce 2D NMs. These three methods only yield small quantities of graphene and as such are not widely utilised in biocatalysis studies using 2D NMs, with the exception of biosensor development.

Liquid exfoliation is the most commonly applied method for larger scale production of 2D NMs. Despite being amenable to larger scale production, liquid exfoliation does not yield 2D NMs with the same level of purity and/or crystalline state as the methods outlined above. In a comprehensive discussion on the exfoliation of 2D NMs in liquids, Nicolosi et al outlined the four techniques currently used to isolate or synthesise 2D NMs: Oxidation followed by dispersion, intercalation, ultrasonication and ion exchange.¹⁶ The oxidation strategy uses concentrated acids to oxidise the surface of the 3D counterpart of the desired 2D NM, causing both exfoliation and modification of the surface with oxygen functional groups. The oxidised surface is then reduced to near pristine 2D NMs in a colloidal form using a suitable reducing agent, such as hydrazine, sodium borohydride or L-ascorbic acid (L-AA). Liquid exfoliation is widely applied for producing GO and

chemically reduced graphene oxides (CRGOs).^{44, 45} The other synthesis approaches require breaking the bonds between the interlayers of the graphite. Intercalation uses *ionic species, for example, sodium dodecyl benzene sulphonate, n-butyllithium and iodine monobromide*, which form inclusion complexes between the exfoliated graphene sheets to reduce their interlayer binding energy.⁴⁶⁻⁴⁹ Further treatment with sonication or thermal shock results in highly exfoliated sheets of graphene that are 1-3 layers thick. This method has been used for the formation of graphene as well as other 2D NMs, such as MoS₂.⁴⁷⁻⁴⁹ The major disadvantage of this method is that it is highly sensitive to any change in ambient conditions with respect to temperature and pH.

The use of ultrasonic waves to exfoliate 2D NMs in solvents is a strategy that has become more common place in recent times.⁵⁰ These waves create cavitation bubbles between the interlayers and weakens van der Waals interaction between them. The surface energy of the solvent needs to be greater or equal to that of the 2D NMs interlayer energy forces.⁵⁰ This results in a simple exfoliation protocol for the production of 2D NMs from their source. Solvents such as N-methyl-pyrrolidone and dimethylformamide have been used for the exfoliation of graphene and hexagonal-BN sheets.⁵¹⁻⁵³ Ion exchange is used in conjunction with ultrasonication to produce 2D NMs from materials which possess exchangeable interlayer ions in their framework, such as LDHs (brucite), clays (vermiculite) and metal oxides (titanium dioxide).^{54, 55} This method uses counterions which replace the interlayer ions, causing electrostatic repulsions which results in expansion of the interlayer space. Subsequent ultrasonication then completes the exfoliation process. Examples of counterions used include dodecyl sulphates to replace interlayer cations in LDHs,⁵⁶ water replacing sodium in clays⁵⁷ and tetrabutylammonium displacing anions in metal oxides.⁵⁴

The 2D NMs synthesised using the methods outlined above possess properties favourable for enzyme immobilisation. These properties can be further modified to change the attributes of the bound enzymes. These properties and functionalisations will be discussed below.

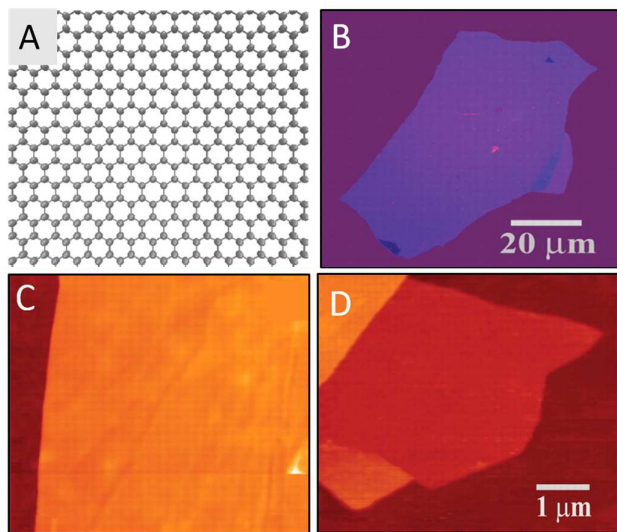
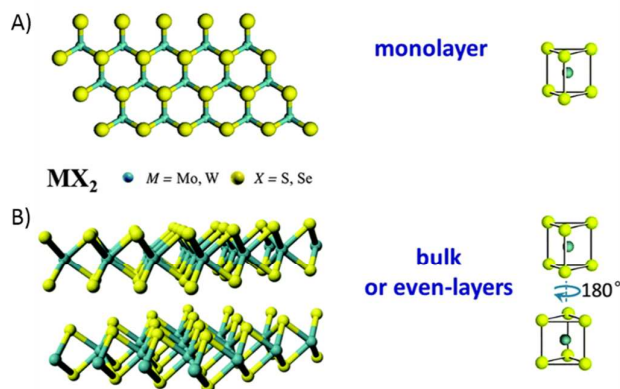


Fig. 1 Graphene flakes visualised as a (A) schematic representation of hexagonal arranged of carbon atoms, (B) multilayer graphene flake with a thickness of ~ 3 nm on top of an oxidised Si wafer. (C) Atomic force

microscopy (AFM) image of a 2 by 2 μm area of a flake near its edge, SiO₂ surface (dark brown) and a flake (orange) 3 nm in height and (D) an AFM image of monolayer of graphene. Reproduced (adapted) from ref ¹ with permission from The American Association for the Advancement of Science.

2.2 Transition metal dichalcogenides

Following their successful isolation of graphene, Novoselvo et al applied their technique to isolate other 2D NMs, such as TMDs.³⁸ The structure of these materials resembles that of graphene, except that the carbon is replaced by a metal (M) atom covalently linked between two chalcogens (X) atoms, in the form of MX₂.³⁸ A family of group-VI TMDs such as molybdenum disulphide (MoS₂), molybdenum diselenide (MoSe₂), tungsten disulphide (WS₂) and tungsten diselenide (WSe₂) share a similar structural morphology



(Figure 2).

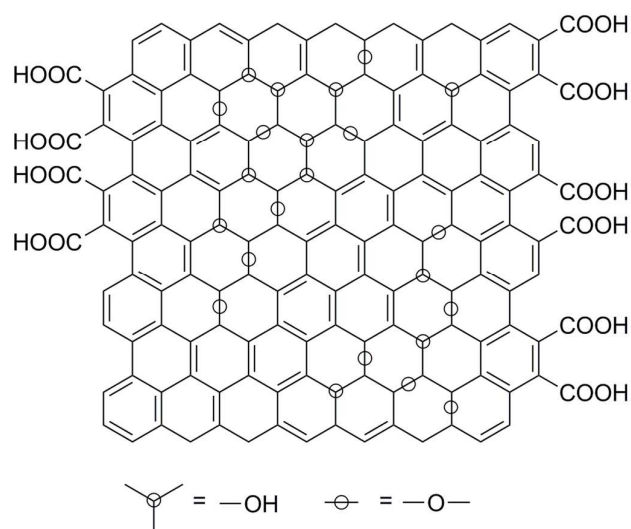
Fig. 2 Schematic of the lattice structure of bulk and monolayer transition metal dichalcogenides (TMDs). (A) Top view of a monolayer TMD crystal (left) and the unit cell (right). (B) Schematic of bulk or even-layer MX₂ structures (left) and the unit cell (right). Reproduced (adapted) from ref ⁵⁸ with permission from Royal Society of Chemistry.

In a TMD monolayer the metal atom is covalently linked to six chalcogens in a trigonal-prismatic coordination that allows the metal to lie at the centre of the prismatic unit cell (Figure 2). The interlayer distance between bilayer TMDs is ~ 0.65 nm, which is higher than that of bilayer graphene (~ 0.33 nm), where the adjacent layers are connected via weak van der Waals forces at 180° planar rotation.⁵⁸ The surface chemistry of TMDs can be modified to give a variety of crystalline phases with distinct electronic properties, such as 1T, 2H and 3R.⁵⁸ Chow et al stated that the surface-surface hydrophobicity of 2–3 layers of TMDs is ~ 83 – 90° . Like graphene, these structures can be tuned to become more hydrophilic via oxidation.⁵⁹

2.3 Properties of graphene and derivatives

Novoselvo et al demonstrated that the mechanical exfoliation of graphite yielded pristine graphene and that a monolayer of graphene is atomically thin with hexagonally arranged sp² hybridised carbon atoms (Figure 1).¹ The presence of sp² domains adds hydrophobicity to graphene with a water contact angle in the order of 90–100°, as reported by Taherian et al.⁶⁰ The graphene

surface can be tuned with concentrated acids to modify the level of oxidation. This allows the synthesis of graphite oxide, which is now known as graphene oxide (GO). There are several different methods for oxidising the surface of graphene, but the most commonly used are the Brodie's, Staudenmaier, and Hummer-Offeman methods.^{45, 61, 62} Each of these methods have their own pros and cons, as discussed by Boehm and Scholz.⁶³ They found that Brodie's method produced the most stable and pure forms of GO. They also noted that compared to the other approaches, the Hummer-Offeman method gave the lowest carbon:oxygen (C/O) ratio, resulting in a high degree of oxidation on the GO surface. As a result of the surface oxidation, the GO contains functional groups such as epoxy (C-O-C), hydroxyl (-OH), carboxyl (-COOH) and carbonyl groups (C=O), as shown in Figure 3.⁶⁴ The oxidised area on the surface of graphene results in sp^3 hybridisation of the carbon orbitals. The surface functionalisation with oxygen groups shields the

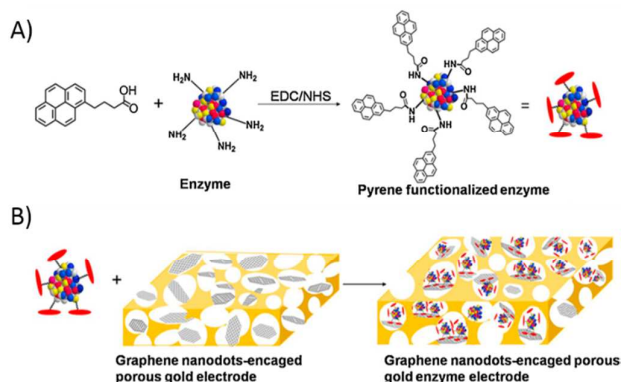


hydrophobic domains of graphene making the surface more hydrophilic, which is highly useful for the physical adsorption of biomolecules.⁶⁵ These 2D graphene derivatives can be easily dispersed in large quantities in a colloidal form and used for applications such as enzyme immobilisation. Established structural models of 2D graphenes possess key surface features that make them useful for enzyme immobilisation, the hexagonal lattice and presence of hydrophobic/hydrophilic domains.

Fig.3 Structural model of graphene oxide.

2.3.1 Hexagonal lattice

Hexagonal lattices in 2D NMs can be useful for immobilising enzymes, as it is favourable for the formation of π - π stacking interactions. Enzymes containing numerous aromatic residues can interact with the surface via these interactions. Further to this enzymes can also be functionalised with polycyclic aromatic groups to increase the strength of these interactions. Recently, Wang et al modified the surface of the enzymes catalase and glucose oxidase (GOx) with pyrene and subsequently immobilised them on graphene nanodots, as shown in Figure 4.⁶⁶ First, 1-ethyl-3-(3-dimethyl-aminopropyl) carbodiimide hydrochloride (EDC) and N-

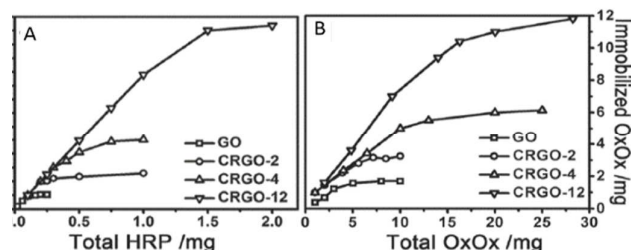


hydroxysuccinimide (NHS) were used to functionalise the surface of the enzymes with a pyrene hydrocarbon. The pyrene-functionalised enzyme was then incubated with graphene nanodots. Due to the presence of similar hexagonal geometries in both the modified enzyme and graphene nanodots, the molecules formed a supramolecular assembly via π - π stacking, allowing the enzyme to be non-covalently bound to the nanodot surface.⁶⁶

Fig. 4 Schematic of the immobilisation of pyrene-functionalised enzyme on graphene nanodots. (A) Pyrene functionalisation of enzyme (glucose oxidase/catalase), followed by (B) incubation with graphene nanodots encaged in a porous gold electrode where immobilisation of the enzymes occurs via π - π stacking. Reproduced (adapted) from ref⁶⁶ with permission from Elsevier.

2.3.2 Hydrophobic domains

Hydrophobic domains are prominent features on the surface of pristine 2D NMs, but are partially concealed once the surfaces have been functionalised. This surface hydrophobicity enables non-covalent interactions to occur, such as physical adsorption. As many enzymes possess hydrophobic domains in their protein structures, it is possible to physically adsorb them onto 2D NMs. Work by Zhang et al demonstrated the physical adsorption of enzymes onto CRGOs via hydrophobic interactions.⁶⁷ Firstly, they altered the surface of GO by controlling the extent of chemical reduction with L-AA, with longer reduction times increasing surface hydrophobicity. Using the CRGOs with varying levels of surface hydrophobicity they investigated how this affected enzyme loading. As shown in Figure 5, hydrogen peroxidase (HRP) and oxalate oxidase (OxOx) were adsorbed (or loaded) onto the CRGOs, with loading increasing as the surface hydrophobicity of CRGOs (-2<-4<-12 hours) increased. However, the loading capacity was selective with respect to enzyme, with the CRGOs able to bind more OxOx (12 mg mg^{-1}) than HRP (1.3 mg mg^{-1}). Similar techniques have been applied across different enzyme classes to immobilise them onto 2D NMs. This will



be discussed in Section 3.

Fig. 5 Immobilisation of the enzymes horseradish peroxidase (HRP) and oxalate oxidase (OxOx) on chemically reduced graphene oxides (CRGOs) of varying hydrophobicity. (A) HRP and (B) OxOx loading on graphene oxide (GO) and CRGOs as a function of the total amount of enzyme. Weights of GO and CRGOs 1 mg. Reproduced from ref ⁶⁷ with permission from John Wiley and Sons.

2.3.3 Hydrophilic domains

Oxidised 2D NMs show a high degree of hydrophilicity on their surface due to the presence of functional groups (noted in Section 2.2). In their colloidal state, deprotonation of these functional groups imparts a negative charge onto the 2D NMs. In this state NMs remain stable across a wide pH range from 2 to 10.²⁶ This property is often used for immobilising enzymes via electrostatic interactions. When using this technique it is essential that the isoelectric point (pI) of the target enzyme is known, so that the pH of the colloidal solution can be controlled and immobilisation on the negatively charged graphene oxide can proceed. As Mathesh et al showed, variation in pH can have significant effects on the immobilisation of HRP (pI 7.2) and GOx (pI 4.2) on GO and CRGOs.⁶⁸ In their experiment, they showed that GO tended to undergo electrostatic interactions with enzymes, while CRGOs led to hydrophobic interactions. They demonstrated this by studying the interaction at different pH. At pH lower than their respective pIs both HRP and GOx attained a net positive charge and underwent electrostatic interaction with the negatively charged GO. As the pH increased the positive charge on the surface of enzymes decreased, resulting in repulsion from GO and decreased loading. In contrast, interaction with CRGOs had no effect on enzyme loading across a wide range of pH values. This suggests that the hydrophobic moieties in the enzyme structures

were adhering to the graphitic regions on the CRGOs.⁶⁸ Through the examples provided above it can be seen that the surface chemistries of 2D NMs, with respect to how they are fabricated, their hexagonal lattice, hydrophilicity and hydrophobicity, have a significant impact on enzyme immobilisation. Graphene derivatives and TMDs have been applied in a large number of enzyme immobilisation studies. Their 2D structural morphologies are discussed in the following sections.

3. Enzymes and the strategies used to immobilise them on 2D NMs

Over the last 5 years there have been numerous studies of enzyme immobilisation on graphene and other 2D NMs. In the past a lack of experimental evidence at a molecular level has resulted in ambiguity in our ability to predict the effect of immobilisation on enzymes and their activity/selectivity towards substrates. A review by Rodrigues et al highlights some of the factors that can contribute to changes in enzyme activity.⁶⁹ The use of 2D NMs as immobilisation supports enables the use of a range of analytical techniques, such as atomic force microscopy, not applicable to studying enzymes bound to micro- and macro-supports. These can shed light on immobilisation mechanisms. A range of different enzyme classes have been immobilised (Table 1) on 2D NMs for a variety of different applications. Most studies have attempted to control and modulate enzyme activity, selectivity, specificity, stability and reusability on 2D NMs. Immobilisation has been achieved by either non-covalent (via physical adsorption and ionic interaction) or covalent (via cross-linking) approaches.²² The following sections provide further detail about the strategies implemented in the immobilisation of enzymes (as listed in Table 1) on 2D NM-based matrices.

Table 1. Examples of enzymes that have been immobilised on 2D NMs

Enzyme	Source	Enzyme class	Immobilisation via	Application	Ref.
D-Psicose 3-epimerase	<i>Agrobacterium tumefaciens</i>	5.1.3.30	Hydrophobic van der Waals	Biocoverison	70
β -Glucuronidase	<i>Penicillium purpurogenum</i>	3.2.1.31	Adsorption	Biotransformation	71
Laccase	<i>Rhus vernicifera</i> <i>Aspergillus oryzae</i> <i>Trametes versicolor</i>	1.10.3.2	Ionic Covalent Non-covalent Encapsulation Entrapment Electro-immobilisation	Biocatalyst Biofuel cell Biosensors	72-79
Trypsin	<i>Bos Taurus</i> & <i>Sus scrofa</i> (pancreas)	3.4.21.4	Ionic Hydrogen bonds	Bio-imaging Biocatalyst	80-82
β -Galactosidase	<i>Cicerarietinum</i> <i>Aspergillus niger</i>	3.2.1.23	Covalent	Lactose reduction	83
Nuclease	<i>Penicillium citrinum</i>	3.1.31	Ionic Hydrophobic	Nucleotide reduction	84

Journal Name					ARTICLE
Peptide N-glycosidase F	<i>Flavobacterium meningosepticum</i>	3.5.1.52	Covalent	Fast detection of N-glycan (polysaccharides)	85
Horseradish peroxidase	<i>Armoracia rusticana</i>	1.11.1.7	Electro deposition Covalent Non-covalent Hydrophobic Ionic	Immunosensor for bacterial detection Biosensor Biocatalysis Biomedicine	68, 75, 86-97
Acid pectinase	<i>Aspergillus niger</i>	3.2.1.15	Cross-linking	Hydrolysis of pectic acid	98
β -Amylase	<i>Trigonella foenum-graecum</i>	3.2.1.2	Covalent	Biocatalyst	99
Tyrosinase	<i>Agaricus bisporus</i>	1.14.18.1	Covalent cross-linking Ionic Hydrophobic electro-immobilisation	Phenolic compound remediation Biosensor	79, 100, 101
Glucoamylase	<i>Aspergillus niger</i>	3.2.1.3	Covalent Non covalent	Biocatalyst, Bioconversion	102, 103
Cellulase	<i>Bacillus subtilis</i>	3.2.1.4	Covalent	Biocatalyst	104
Phytase	<i>Bacillus subtilis</i>	3.1.3.8	Covalent	Biocatalyst	105
Lysozyme	<i>Micrococcus lysodeihiticus</i>	3.2.1.17	Adsorption	Biocatalyst	106
α -Chymotrypsin	<i>Bos taurus</i> (pancreas)	3.4.21.1	Ionic Covalent Hydrophobic	Protein inhibitor Biocatalyst Enzyme inhibitor	107-109
Cytochrome C	<i>Equus caballus</i> (heart)	1.1.2.8	Ionic Hydrophobic	Biocatalysis	110
Cholesterol oxidase	<i>Streptomyces Sp.</i>	1.1.3.6	Electro-deposition	Biosensor	88
Topoisomerase I	<i>Homo sapiens</i> (expressed in <i>Saccaromyces cerevisiae</i>)	5.99.1.2	Covalent	Enzyme detection in crude samples	111
Lipase	<i>Rhizopus oryzae</i> <i>Candida rugosa</i> , <i>Penicillium camemberti</i> <i>Alcaligenes Sp.</i> <i>Candida antarctica</i>	3.1.1.3	Covalent Adsorption Ionic Cross-linking	Biocatalyst	112-116
Esterase	<i>Bacillus subtilis</i> <i>Pyrobacterium calidifontis</i> <i>Geobacillus thermoleovarans</i>	3.1.1.1	Covalent Adsorption	Biocatalyst	116
Microperoxidase-11	<i>Equus caballus</i> (heart)	1.11.1.7	Entrapment	Biosensor	117
Oxalate oxidase	<i>Hordeum vulgare L.</i>	1.2.3.4	Adsorption	Biosensor	118
Polyphenol oxidase	<i>Agaricus bisporus</i>	1.10.3.1	Covalent	Biosensor	119

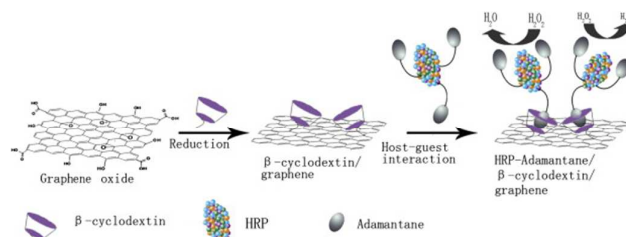
Naringinase	<i>Aspergillus niger</i>	3.2.1.40	Adsorption	Biocatalyst	120
Urease	<i>Canavalia ensiformis</i>	3.5.1.5	Layer by layer assembly	Biosensor	121
Acetylcholinesterase	<i>Electrophorus electricus</i>	3.1.1.17	Adsorption	Biosensor	122, 123
Proteinase K	<i>Tritirachium album</i>	3.4.21.64	Ionic	Biocatalyst	82
Catalase	<i>Bos Taurus</i> (liver)	1.11.1.6	Adsorption π - π interaction	Biosensors	66, 124
Glucose oxidase	<i>Aspergillus niger</i> <i>Myrothecium verrucaria</i>	1.1.3.4 1.3.3.5	Non-covalent	Biocatalyst	66, 89, 94, 103,
			Covalent	Bioconversion	125-145
			Entrapment	Biofuel cell	66, 68, 78, 127,
			Ionic	Biomedicine	146-153

3.1 Non-covalent immobilisation

Non-covalent immobilisation provides the most straight forward approach to attaching enzymes onto 2D NMs. It involves mainly physical adsorption/deposition via hydrogen bonds, van der Waal forces, hydrophobic and electrostatic interactions. These forces are generally weaker than covalent bonds and are formed based on their ability to attract through dipole-dipole forces, intermolecular forces, similar surface residues and opposing surface charges between enzyme and matrix. The following section highlights different examples of enzymes that have been non-covalently bound to graphene and graphene derivatives which have been functionalised using a range of approaches.

The first non-covalent immobilisation of an enzyme on unmodified graphene was the physical absorption of GOx, of interest because of its application in glucose sensors.¹⁴⁶ The bound GOx was found to retain its native conformation and exhibited direct electron transfer from the active site to the graphene electrode surface. This is perhaps the simplest fabrication and immobilisation of GOx onto a graphene electrode. Zhang et al developed a novel layer by layer (LBL) method to functionalise the surface of graphene for GOx immobilisation.¹³⁹ This involved the surface being functionalised with two water soluble functional groups, copper phthalocyanine-3,4',4'',4'''-tetrasulfonic acid tetrasodium salt (TSCuPc) and an alcian blue pyridine variant (AB). The two functionalised graphenes were assembled together through alternating electrostatic interactions. This was achieved by functionalising the glassy carbon electrode with negatively charged sulfanilic acid to immobilise the positively charged graphene-TSCuPc (GR-TSCuPc), over which the negatively charged graphene-AB (GR-AB) was assembled. This modification allowed the positively charged GR-AB to interact with the negatively charged GOx. As discussed in section 2.3, GOx has also been immobilised by modifying the structure with pyrene functionalities to facilitate π - π stacking interactions on graphene nanodots. Das et al and Qu et al immobilised GOx via electrostatic interactions and physical adsorption on graphene modified with metal nanoparticles for use in biofuel cells.^{77, 137} When the nanoparticles were closely packed on graphene the enzyme loading capacity and electron transfer kinetics was improved.

The first non-covalent immobilisation of HRP on GO was carried out by Zhang et al through electrostatic interaction.⁹⁶ The immobilisation was studied at different pH values with pH 7 resulting in the most efficient immobilisation. Following this initial study a detailed analysis of the stability and catalytic activity against different phenolic substrates was performed.⁹⁵ Immobilisation of HRP on GO was favoured by the enzyme's surface functional groups, but on graphene the immobilisation was inefficient, requiring the addition of linkers. For example, sodium dodecylbenzenesulfonate (SDBS) was used to functionalise graphene to impart a negative charge on the surface, which enabled the immobilisation of HRP via electrostatic interactions.⁹² A novel immobilisation technique using host-guest supramolecular interactions has also been demonstrated between HRP and GO.⁸⁷ This involved the surfaces of both being modified, as shown in Figure 6. The GO is functionalised with the natural polymer beta-cyclodextrin (β -CD) and subsequently reduced to β -CD-graphene in



the presence of hydrazine (reducing agent), while HRP is covalently functionalised with the chemical group adamantane. Both of these complexes then undergo supramolecular host-guest interactions to form a nanobiocomposite with utility in the detection of hydrogen peroxide.⁹²

Fig. 6 Schematic representation of the fabrication of the HRP-ADA/CD-graphene/GC electrode and the principle for H_2O_2 determination. Reproduced from ref⁸⁷ with permission from Elsevier.

Immobilisation of HRP on reduced graphene oxide (rGO) was taken a step further by introducing the magnetic particle Fe_3O_4 (Figure 7).⁷⁵ Different percentages of iron content on GO were studied as matrices for HRP immobilisation, with each reduced to Fe_3O_4 -rGO (with varying percentages of Fe_3O_4). When compared with free HRP, rGO or Fe_3O_4 , it was found that composites containing high percentages of Fe_3O_4 provided improved adsorption

of HRP, increasing the enzyme's activity and stability. This technique was also implemented in the immobilisation of laccase, with the same advantages being apparent.⁷⁵

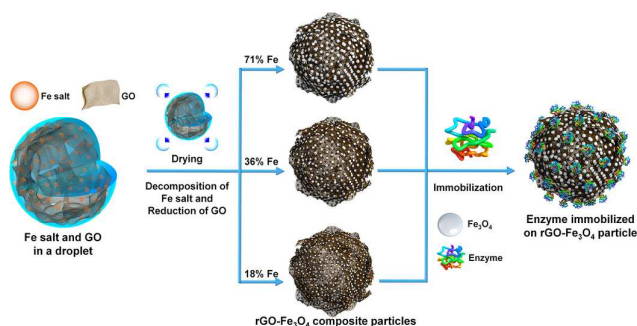


Fig. 7 Schematic diagram for the synthesis and immobilisation of an enzyme on rGO-Fe₃O₄ composite particles. Reprinted with permission from ref.⁷⁵. Copyright 2017 American Chemical Society.

Laccase (from *Rhus vernicifera*) was immobilised on GO via electrostatic interactions for the purpose of quantifying extracellular oxygen released by human erythrocytes.⁷² This used 2,2'-azino-bis(3-ethylbenzothiazoline-6-sulfonic acid (ABTS) as a redox mediator integrated between laccase and GO. The surface of GO was functionalised with ABTS through π - π stacking interactions, imparting a net negative charge on the surface allowing for the electrostatic adsorption of the enzyme.⁷² Another laccase (from *Trumpets versicolor*) was immobilised on a novel support utilising copper-phosphate crystals, GO and carbon nanotubes (CNT) to form a self-assembling 3D nanoflower hybrid composite, as shown in Figure 8.⁷⁶ This is a one-pot immobilisation strategy to attach laccase onto the 3D microcomposite, in which all of the components are mixed and incubated together.⁷⁶

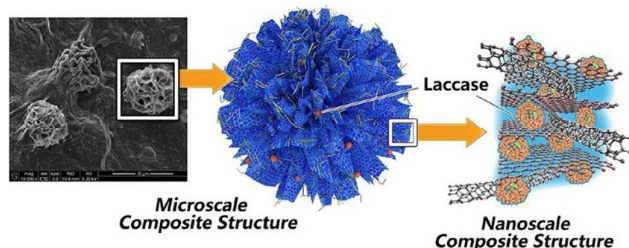


Fig. 8 A 3D flower-like structure formed through the self-assembly of a hybrid nanocomposite of graphene oxide, carbon nanotubes, copper phosphate and laccase (from *Trumpets versicolor*). Reproduced from ref.⁹¹ with permission from Elsevier.

The composite was formed primarily through the coordination of the amine backbone of laccase with copper-phosphate crystals, creating laccase-copper phosphate lamellae. The individual lamella then self-assembled via protein-protein interactions between laccase on neighbouring lamellae to form a flower-like structure. CNT and GO were incorporated together within the microcomposite through electrostatic interactions in the presence of copper ions. In the finished composite the CNTs intertwine with the lamellae and

act as interlayer spacers between GO sheets. The GO also encapsulated the laccase, preventing interaction between neighbouring enzyme molecules and GO sheets.⁷⁶ The resulting biocomposite exhibited improved enzyme loading capacity and activity when compared with other enzymes (cytochrome c) immobilised on 3D metal organic frameworks.⁷⁶ It is thought that the semi microporous structure and interlayer space between individual laccase molecules facilitates their interaction with substrates and improves activity.⁷⁶

Interfacial activation is a phenomenon commonly associated with lipases, where they tend to exhibit enhanced catalytic activity in the vicinity of hydrophobic surfaces, whether from a substrate or a support. This is because the lid covering the active site of the lipase is usually surrounded by hydrophobic domains that favourably interact with other hydrophobic groups/surfaces. Exploiting this property Mathesh et al immobilised lipase QLM from *Alcaligenes sp.* on CRGOs with different levels of hydrophobicity on their surface.¹¹⁵ The surface hydrophobicity was controlled by reducing the oxygen-containing functional groups on the surface of GO for different lengths of time with L-AA. The resulting CRGOs possessed different levels of hydrophobicity, allowing for the effect of this variable on enzyme catalytic properties to be investigated.

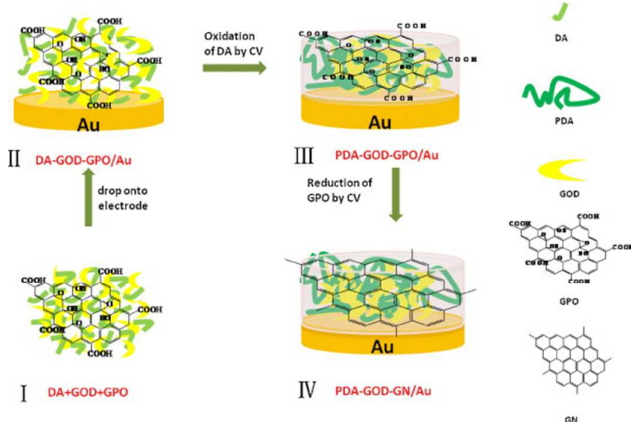
A number of enzymes have been immobilised using physical adsorption through electrostatic, hydrophobic and π - π stacking interactions. Enzymes that have been immobilised by these means include OxOx, cellobiohydrolase, xylosidase, 1-4- β -N-acetylglucosaminidase, D-psicose-3-epimerase, β -galactosidase and tyrosinase.^{101, 118, 154, 155} The immobilisations were carried out without the requirement of surface modification to either the enzyme or 2D NMs. The direct adsorption of these enzymes on 2D NMs has been shown to have a significant effect on both their structure and function

Trypsin is a biologically important proteolytic enzyme that is used as a treatment for pancreatic insufficiency as well as for many industrial and laboratory applications. Understanding interactions between the enzyme and matrix are essential for efficient utilisation of this enzyme in immobilised forms. Jin et al immobilised trypsin on GO which had been modified with polyethylene glycols (PEGs).⁸² Amino terminated PEGs of different lengths (e.g. 2 kDa PEG diamine (2k-I-NH₂-PEG-NH₂) and 10 kDa 6 arm branched PEG (10k-6br-PEG-NH₂) were covalently linked to GO. The positively charged amino terminals on the PEGylated GO were able to electrostatically interact with trypsin.

3.2 Covalent immobilisation

The surface of 2D NMs can be functionalised with epoxy or carboxyl groups. The reactive epoxides can form covalent bonds directly with the enzyme through its N-terminal. Alternatively various combinations of peptides and crosslinking agents can be used to attach enzymes through their C-terminal or sidechains. Although covalent interaction is very stable and removes the problem of enzyme leaching, the site(s) of covalent attachment may have significant effects on the enzyme structure and activity and do not allow for recovery of the enzyme from the support. Wu et al electrosprayed a mixture of PVA, glutaraldehyde and graphene to form a stable biocompatible matrix for GOx immobilisation.¹⁵³

Electro-grafted polymer from *N*-succinimidyl acrylate (NSA) has also been applied to covalently bond GOx to electrochemically reduced graphene oxide.¹⁴⁸ Similarly Ruan et al used dopamine (DA) and GO to immobilise GOx.¹³¹ DA, GO and GOx were mixed together and dropcast onto a gold electrode and then electrochemically oxidised (Figure 9). As a result DA polymerised to form poly-DA (PDA) and GO was reduced concomitantly, with PDA acting as a cross-linker to attach GOx to GO.¹³¹ The above methods describe three different approaches to covalently bind GOx to polymer-modified graphenes. Although all of the methods result in direct electron transfer from the active redox centre of the enzyme to the electrode surface, they differ in the simplicity of the biosensor fabrication. PDA is the simplest of the three, and provides an inexpensive and green strategy to fabricate a glucose biosensor using 2D graphenes. The polymer chitosan has been applied as a cross-linker to immobilise GOx to graphene modified electrodes. Chitosan functions by cross-linking amino acids on the enzyme surface, improves



biocompatibility and the ability to form films, and modifies the surface properties of graphene and GOx. For example, when nitrogen-doped graphene is incorporated into a chitosan matrix,^{126, 135} GOx absorption is enhanced and imparts a net positive charge to the bionanocomposite at pH below the molecules pI. This makes the assembly of the bionanocomposite on the electrode surface simpler and more efficient.^{126, 135}

Fig. 9 Schematic representation of the process of immobilising glucose oxidase on graphene crosslinked with poly-dopamine, on a gold electrode. Reproduced from ref¹³¹ with permission from Elsevier.

Covalent immobilisation of GOx was also investigated on other 2D NMs. Su et al replaced graphene with MoS₂ and covalently cross-linked GOx onto gold-modified MoS₂ (AuNp/MoS₂) using Nafion™.¹⁵⁶

A novel hydrogen peroxide biosensor with Au NPs and chitosan was developed by Zhou et al.¹⁵⁷ Graphene and HRP were co-immobilised into a chitosan matrix which showed an excellent electrocatalytic response towards hydrogen peroxide. To further improve the biosensor's sensitivity the immobilisation of HRP was carried out with graphene quantum dots (GQDs) via a peptide amino linkage between carboxyl and amino groups present on GQDs and HRP, respectively.⁹³ The fabrication method used NHS and EDC to activate the -COOH groups before coupling with HRP. The immobilised HRP-GQD was then dropcast onto a glassy carbon

electrode before being incubated with chitosan to securely attach HRP-GQD to the modified electrode surface. A multi-point covalent immobilisation of laccase (from *Trametes versicolor*) on GO was accomplished by Patila et al to form multilayered enzyme-graphene nanostructures.⁷⁴ In this work GO was functionalised with hexamethylenediamine to introduce amino groups on the surface. The laccase was then covalently immobilised using glutaraldehyde as a cross-linking agent. The biocatalytic activity of this composite was measured against industrial pollutants, such as anthracene and pinacynaol chloride (dye), to investigate the degradation of these compounds. The activity of the immobilised material for the degradation of the pollutants increased as the thickness of the nanoassembly increased. These findings show promise for the application of these composites in the removal of industrial pollutants.⁷⁴

A range of different lipases from *Rhizopus oryzae*, *Candida rugosa* and *Penicillium camemberti* have been covalently immobilised on GO to investigate their tolerance in polar protic/aprotic and non-polar solvents, as well as their conversion rate of fatty acids into acylglycerols.¹¹⁴ Hermanova et al. used glutaraldehyde to crosslink lipases with GO prepared by either the Brodie or Staudenmaier methods. Glutaraldehyde was added at different stages in the immobilisation protocol (to the GO dispersion prior to immobilisation, to non-specifically immobilised enzyme on GO and to the GO dispersion simultaneously with the lipase) to investigate how this affected the activity and stability of the immobilised enzyme.¹¹⁴ A lipase from *Yarrowia lipolytica* was covalently immobilised on carboxyl-functionalised GO. The COOH was functionalised through the addition EDC and NHS-facilitated conjugation improving the coupling efficiency between enzyme and GO.¹¹² Amine-functionalised GO has also been used in the covalent immobilisation of lipases and esterases.¹¹⁶

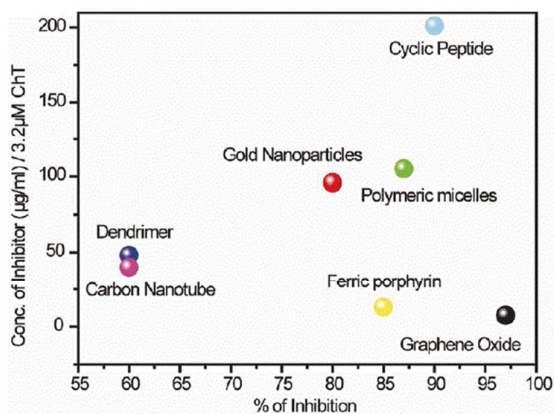
Further to the examples outlined above, a number of other industrially useful enzymes have been immobilised on 2D NMs. Examples include cellulase, alcohol dehydrogenase, nuclease P₁, tyrosinase, beta-glucuronidase, N-glycosidase, urease, D-psicose-3-epimerase, beta-galactosidase, cytochrome C and acetylcholinesterase.^{70, 71, 84, 101, 107, 108, 121, 124, 155, 158} However, compared to enzymes such as GOx, HRP, laccases and lipases the number of works published using these enzymes with 2D NMs is relatively low. Examples of the enzymes β-galactosidase, peptide-N-glycosidase-F (PNGaseF), polyphenol oxidase, cellulase, tyrosinase, glucoamylase phytase covalently immobilised on GO derivatives are also present in the literature. The surface modifications made to GO that allow for the covalent immobilisation of these enzymes are described below. Immobilisation was carried out using thiol-functionalised graphene sheets (β-galactosidase cross-linked by glutaraldehyde), carbodiimide-activated amidation on GO (PNGaseF), Fe₂O₃-polymer (poly(3,4-ethylenedioxythiophene)) functionalised rGO (polyphenol oxidase), magnesium oxide functionalised GO (cellulase), GO (tyrosinase cross-linked by glutaraldehyde or EDC/NHC), cyanuric chloride conjugated F₂O₃-GO (glucoamylase) and Mg NPs conjugated GO (phytase). Most of the above enzymes were immobilised in attempts to improve their performance in biocatalytic and biosensory-related applications.

The incorporation of 2D NMs into aerogels for use in enzyme immobilisation is another rapidly expanding branch of research.

Aerogel matrices have been used for some time, however in most cases the prepared sol-gel conditions are still too harsh for many biomolecules. Recently a graphene/ γ -Fe₂O₃ aerogel was synthesised using a supercritical drying method and produced a matrix with dual functionality.⁷¹ The presence of graphene adds conductivity and increases the rate of electron transfer, while Fe₂O₃ provides a magnetic quality which aids in separation of the matrix from reaction products. This matrix was synthesised by mixing GO, Fe₂O₃.6H₂O and epichlorohydrin together in dimethylformamide. The addition of epichlorohydrin initiated the hydrolysis and polycondensation of Fe₂O₃.6H₂O, which was then dried using supercritical CO₂ and subsequently carbonised at 260 °C in an argon atmosphere. This aerogel precursor was then used to produce either γ -Fe₂O₃ through etching or graphene aerogels through calcination. The synthesised graphene/ γ -Fe₂O₃ was then used to immobilise β -glucuronidase and applied in the biotransformation of glycyrrhizin into glycyrrhetic acid. High enzyme loading of 2.5 mg/mL was achieved and the immobilised material possessed good biocompatibility and high activity.⁷¹

In some instances GO may act as an inhibitor of the enzymes immobilised on it. De et al pioneered studies using GO to strongly inhibit α -chymotrypsin (ChT) (Figure 10).¹⁰⁷ They showed that ChT can undergo electrostatic, hydrophobic and π - π stacking interactions to bind to the surface of GO. These interactions progress from initial electrostatic interactions, and are followed by strong adsorption of the enzyme active site at the interface, due to hydrophobic interactions.¹⁰⁷ It was demonstrated that a 20 μ g/mL concentration of GO was sufficient to completely inhibit the activity of 3.2 μ M concentration of ChT. Interestingly, this interaction is reversible at high salt concentrations, which interferes with the surface charge and nullifies the electrostatic interactions.¹⁰⁷ The mechanisms by which ChT interacts with GO and graphene have been reported in detail using both theoretical and experimental studies.^{107, 109} Sun et al attempted to minimise or remove the inhibitory effect of GO on ChT by functionalising the surface of GO with tripod-binding motifs (Figure 11).¹⁰⁸ Two different tripods (1 and 2) were designed and used to functionalise the surface of GO. It was found that compared to GO, the inhibitory effect was diminished when ChT was immobilised on GO functionalised with the tripods. Comparing immobilisation of ChT on modified and unmodified GO allowed the surface features that affect the activity of ChT to be investigated. They found that the presence of hydrophobic domains on GO significantly deformed the active site of ChT after immobilisation. The functionalisation of GO with tripods effectively provides a spacer between the hydrophobic regions and the active site of ChT, preserving the activity of ChT once immobilised.¹⁰⁸

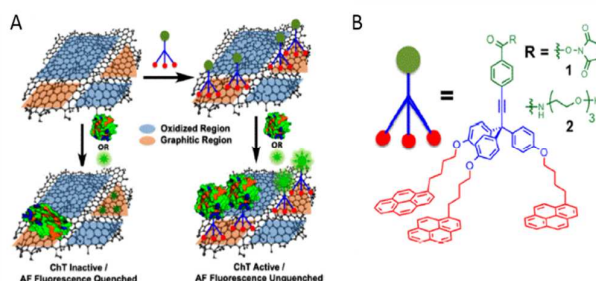
Fig. 10 Degree of α -chymotrypsin inhibition by various nanomaterials



relative to the inhibitor concentration. Reproduced with permission from ref ¹⁰⁷. Copyright 2011 American Chemical Society

In addition to graphene and graphene-based derivatives, research into immobilisation of enzymes with other 2D NMs is also expanding. An example is the work of Nasir et al who used different 1T-phase TMDs, such as MoS₂, MoSe₂, WS₂ and WSe₂, to evaluate their performance in the detection of an organophosphate pesticide (fenitrothion).¹⁵⁸ Acetylcholinesterase (AChE) was immobilised covalently on the TMDs using glutaraldehyde as a cross-linker and then tested for activity. The immobilised AChE interacts with acetylcholine and results in electron transfer to the electrode surface. In the presence of fenitrothion the active site of AChE is irreversibly inhibited and electron transfer ceases allowing detection of the compound. It was found that WS₂ was the most efficient in detecting fenitrothion, most likely due to the high loading capacity (due to the exfoliation using tert-butyllithium) of this material, allowing for more AChE to be bound.

Fig. 11 Schematic showing the functionalisation of graphene oxide (GO) with tripod binding motifs. (A) Model depicting the interaction of chymotrypsin (ChT) and AF 488 to native GO and GO functionalised with tripod 1. ChT activity and AF 488 fluorescence are lost when the hydrophobic regions are solvent exposed (left). Tripod 1 passivates the hydrophobic regions and reacts with primary amines to anchor active ChT and AF 488 to the surface



(right). (B) Structures of the tripods 1 and 2. Reprinted (adapted) with permission from ref ¹⁰⁸. Copyright 2015 American Chemical Society.

4. Modifying enzyme structure and function through immobilisation on 2D NMs

To facilitate the immobilisation of a range of enzymes on 2D NMs, a variety of surface functionalisations have been applied. The interaction of enzyme structures, including specific residue side chains and/or active sites with a solid support is highly dependent on the support's surface features. With this in mind the surface properties of 2D NMs can be tailored to modify and potentially control the biocatalytic activity of different enzymes. Here, we discuss examples of work carried out immobilising different enzymes to GO, GO derivatives and TMDs and how this can contribute to the modification of enzyme structure and function.

4.1 Modulation of enzyme properties

4.1.1 Enzyme conformation

The presence of hydrophilic or hydrophobic domains on support

surfaces can be used to bind enzymes and in some instances modify enzyme structure from its native/unbound conformation. A number of studies using 2D NMs have demonstrated this. The immobilisation of lysozyme on hydrophilic GO and hydrophobic rGO showed that the enzyme's activity was retained on rGO, but inhibited by GO.¹⁰⁶ Lysozyme undergoes multiple interactions with GO, including π - π stacking, hydrophobic interaction, hydrogen bonding, van der Waals and electrostatic forces, which causes lysozyme to flocculate and form long fibre-like structures. Structural characterisation studies revealed that the intrinsic fluorescence of tryptophan (Trp) residues in lysozyme bound to GO and rGO were altered. This showed that the fluorescence was quenched significantly more in the presence of GO (65% decrease in fluorescence compared to free lysozyme) than with rGO (15% decrease). This quenching of intrinsic Trp fluorescence indicated that lysozyme underwent denaturation, exposing Trp residues to the aqueous environment. As Trp62 and Trp63 are close to the active site, these changes may be linked to the loss of activity when lysozyme was bound to GO. The interaction of lysozyme with rGO was significantly lower and therefore impacted activity less.¹⁰⁶

A molecular dynamic study using trypsin and ChT as model enzymes showed that hydrophilic amino acid residues, mainly lysine and asparagine, interacted through strong hydrogen bonds with the epoxy and carboxyl groups of GO.¹⁰⁹ Interaction of a single molecule of ChT covered a large surface area of approximately 12.3 nm² when it was adsorbed onto the surface of GO. However, through the interaction with the rGO surface, the area of absorption of ChT was only 8.6 nm². The α -region on the catalytic site of ChT, known as the S₁ specific pocket, is an important locus for controlling enzyme specificity and efficiency. This region was 18.6 Å away from the graphene surface, but only 7.2 Å away from the GO surface, leading to increased deformation of the ChT active site on GO. The residue sequence of 'TNCKKYW' contained within the α -helix acts as an anchor to fix the enzyme to the surface prior to interaction by active site adsorption on GO (Figure 12). This interaction partially blocks the active site and inhibits the activity of ChT.

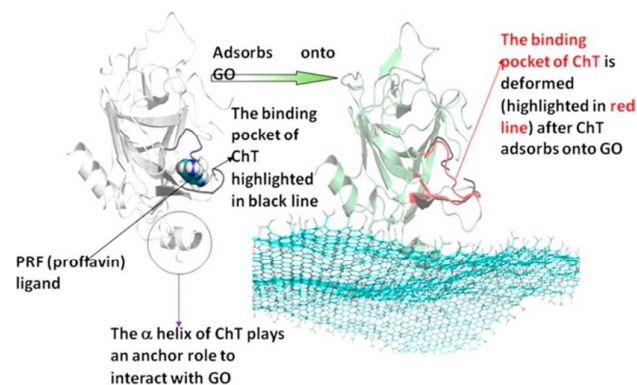
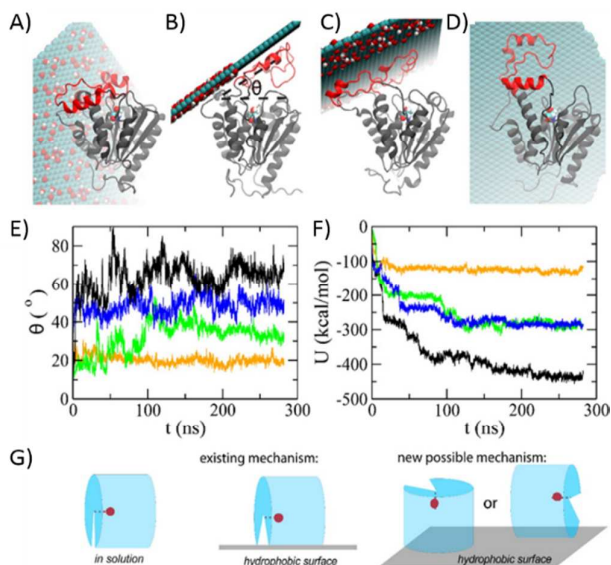


Fig. 12 Molecular dynamic representation of ChT interaction with graphene oxide (GO). Active site of chymotrypsin (ChT) is deformed after ChT is adsorbed onto the surface of GO, as the α -helix of ChT acts as an anchor site interacting with GO. Reprinted with permission from ref¹⁰⁹. Copyright 2012 American Chemical Society.

Pavlidis et al immobilised a range of lipases and esterases onto GO, both covalently and non-covalently, to assess the effect of different immobilisation methods on catalytic behaviour.¹¹⁶ In most instances the enzymes bound non-covalently performed esterification (lipase) and transesterification (esterase) at a higher rate. However, lipase from *C. rugosa* and esterase from *G. thermoleovorans* were more active when covalently immobilised. In addition, covalently bound lipase B from *Candida antarctica* was shown to retain more activity after multiple reaction cycles. A correlation was also seen between enzyme secondary structure (α -helical content) and catalytic activity, with higher activities associated with greater percentages of α -helix. The esterase from *B. subtilis* was an exception to this trend and despite similar percentages of α -helix, was only active when non-covalently bound to GO, showing no activity when covalently bound. These studies



highlight the complexity of understanding how to control these processes and that successful immobilisation relies not only on the properties of the nanomaterial or the immobilisation procedure, but also to the specific properties of different enzymes themselves.

Fig. 14 Conformational and energetic changes of the lipase QLM (from *Alcaligenes Sp.*) upon interaction with graphitic nanosheets. (A) Final conformation of QLM on the GO nanosheet. (B, C) Final conformations of QLM on the GO/GR1 and GO/GR2 nanosheets, respectively. (D) Final conformation of QLM on the GR nanosheets. (E) Angles between the lipase lid and support surface after QLM adsorption onto different nanosheets. (F) Time-dependent interaction energies between QLM and the graphitic nanosheets (yellow, GO; green, GO/GR1; blue, GO/GR2; black, GR). (G) Proposed mechanism for the enhanced activity of QLM on a hydrophobic support: adsorption facilitates side-on substrate access to the QLM active site. The active site inside the QLM (transparent and cyan) is depicted as red dot. Reprinted (adapted) with permission from ref¹¹⁵. Copyright 2016 American Chemical Society.

As discussed in section 3.1, lipases undergo interfacial activation in the vicinity of hydrophobic interfaces. As such, 2D NMs with hydrophobic surface properties, such as GO/CRGOs, can be used to physically adsorb lipases. Lipase activity can be partially controlled

or modified by tuning the surface of GO to give CRGOs of varying hydrophobicities.¹¹⁵ Non-covalently immobilised lipase QLM (*Alcaligenes sp.*) on CRGOs of varying hydrophobicities was reacted with lipid substrates (olive oil and p-nitrophenol palmitate). The activity increased as surface hydrophobicity was increased to a point (CRGO reduced for 4 h), before decreasing with more hydrophobic surfaces. Trajectory molecular dynamic simulation studies showed a detailed interaction of lipase QLM on the hydrophilic (GO), partially hydrophilic (GO/GR1), partially hydrophobic (GO/GR2) and hydrophobic (GR) surfaces (Figure 14). It was observed that the lipase lid interacted with the hydrophobic domain on all surfaces. For GO the hydrophobic lid was pinned and little mobility was observed on the surface. But as the surface hydrophobicity increased the lipase showed more mobility due to increased hydrophobic interaction. The lipase interacted with hydrophilic or partially hydrophobic (GO/GR1/GR2) surfaces, i.e. it adsorbed either on edges or moved to hydrophobic domains before completely binding with the surface (Figure 14B/C). CD and ATR-FTIR spectroscopy showed changes in secondary structure with a transition from α -helix to β -sheet as the surface hydrophobicity increased.¹¹⁵ Unlike the study by Pavlidis et al, this work showed that the decrease in α -helix can result in an increase in activity and further emphasises how specific enzymes can react differently with 2D NMs.

4.1.2 Enzyme activity, selectivity and stability

In an attempt to improve the activity, selectivity and stability of various enzymes, the surface chemistry of 2D NMs can be modified with suitable functional groups. However, these approaches may vary with respect to different enzyme classes and cannot be generalised. Some of the enzymes immobilised on unmodified and modified 2D NMs to enhance the above enzyme properties are discussed below.

A lipase from *Yarrowia lipolytica* was covalently immobilised on carboxyl-functionalised GO.¹¹² Hydrolysis of olive oil at 40 °C showed that the immobilised lipase retained 80% activity in aqueous media compared to the free lipase. This decrease in activity was attributed to changes in the secondary structure of the bound enzyme, with 73.6% α -helix content retained relative to the free enzyme. In non-aqueous conditions the activity of the immobilised lipase was found to be higher. The enantiomeric resolution of (R,S)-1-phenylethanol by both immobilised and free lipase was compared in heptane, with (R)-1-phenylethanol converting to (R)-1-phenylethyl acetate when reacted with vinyl acetate, while (S)-1-phenylethanol is unchanged. The catalytic efficiency (k_{cat}/K_m) of the immobilised lipase to resolve the racemic mixture was 1.6-fold higher than that of the free lipase.

This work demonstrates that immobilisation of lipase on GO has the ability to improve the specificity and catalytic rate at which the enzyme carries out reactions. Hermanova et al investigated the effect of non-covalently and covalently binding lipases from *Rhizopus oryzae*, *Candida rugosa* and *Penicillium camemberti* to GO and assessing the enzyme activity and stability in a range of solvents.¹¹⁴ They found that lipase from *R. oryzae* was the most active in carrying out an esterification reaction for the formation of acylglycerols with a range of fatty acid chain lengths. *R. oryzae* lipase retained the highest activity of the three lipases when tested

in different solvent types, displaying the highest selectivity in polar aprotic (acetone) and protic (isopropanol) solvents. Other work by the group using *R. oryzae* lipase demonstrated improved thermal and solvent stability of the enzyme when immobilised on GO.¹¹³ Importantly they showed that the methods by which GO is prepared (Brodie or Staudenmaier methods) and the order of steps in the immobilisation protocol (i.e. when/if glutaraldehyde is added) influence the activity and stability of the bound enzyme. They determined that for applications in organic solvents simple physical adsorption was the optimal procedure.

D-Psicose (epimer of D-fructose) is a relatively rare sugar that plays important physiological roles in the body. Production of the compound by enzymatic means is possible using ketose 3-epimerases, however the reaction often has low bioconversion efficiency. Dedania et al immobilised D-psicose 3-epimerase from *Agrobacterium tumefaciens* onto GO via physical adsorption and then investigated the enzyme's activity and reusability.⁷⁰ They found that while the pH optima of the immobilised enzyme changed only a minor amount to pH 7.5 (pH 8.0 for the free enzyme), the temperature optima increased to 60 °C, compared with 50 °C for the free enzyme. As well as an increase in optima, the enzyme's thermal stability improved significantly with immobilisation on GO. At 60 °C the bound enzyme had a half-life of 720 min, compared to 3.99 min for the free enzyme. As an immobilisation material GO also provided a greater improvement in thermal stability compared with other materials that have been used to immobilise ketose 3-epimerases, such as Duolite™ A568 and artificial oil bodies. The rate which the immobilised D-psicose 3-epimerase carried out the bioconversion of D-fructose to D-psicose was also improved, producing 4 mM D-psicose from 10 mM D-fructose after approximately 250 min, compared to 3.2 mM for the free enzyme.

Immobilisation of HRP onto GO (GO-HRP) via electrostatic interaction (and testing for its ability to oxidise and remove phenolic compounds from solution), resulted in GO achieving higher loading of HRP (100 mg of HRP/g of GO) than seen for numerous macro-support materials, primarily due to the large surface area.⁹⁵ The pH optima of the bound enzyme remained unchanged at pH 7.0. However, the immobilised HRP was found to have an improved stability over a wider range of pH, with 36% of activity retained at pH 10, compared to 10% for the free enzyme. Thermal stability was also improved notably at 50 °C, where after 20 min incubation the bound and un-bound enzyme retained 72 and 28% of activity, respectively. These changes suggest that by binding HRP to GO the enzyme is better protected from heat-induced denaturation. Further to the above improvements, GO-HRP also exhibited improved storage stability over 40 days, retaining 56% activity compared to 12% for the free HRP. The ability of bound and free HRP to remove seven different phenolic compounds from aqueous solutions was compared. For five of the seven compounds removal efficiency was relatively unaffected by immobilisation, with efficiencies in the range of approximately 55–90% achieved. However, free HRP was poor at removing 2-chlorophenol (16.1%) and 2,4-dimethoxyphenol (17.6%), with immobilisation on GO improving removal efficiency. The removal of 2,4-dimethoxyphenol was carried out with two times higher efficiency (34.4%) by GO-HRP and 2-chlorophenol removal was improved moderately (20.4%),

compared with free HRP. This result indicates that by binding HRP to GO the enzyme's selectivity for the oxidation of certain phenolic compounds is improved. Zhang et al suggested that the improvement toward ortho-substituted phenols may be due to structural confirmation changes caused by immobilisation on GO.

Serine proteases trypsin, chymotrypsin and proteinase K were immobilised on GO.⁸² However, it was found contrary to expectation that binding the proteases on GO severely diminished their activity. Jin et al used amino-terminated PEGs to functionalise GO to try and improve the activity of bound trypsin (Figure 13).⁸² They observed that modification of GO with either 2k-I-NH₂-PEG-NH₂ (2 kDa) or 10k-6br-PEG-NH₂ (10 kDa) resulted in the nano-interface of GO altering the activity of bound trypsin. The activities of all three proteases were improved to free enzyme-like levels or better. The activity of trypsin bound on PEGylated-GO was significantly improved against casein (up to 2-fold higher than free trypsin). The presence of the PEG polymers played an important role in blocking the hydrophobic domains on GO, preventing their direct interaction with the enzyme's active site. In addition to increased activity with casein the bound trypsin displayed selectivity. Other proteolytic substrates such as haemoglobin, bovine serum albumin (BSA) and N α -p-tosyl-L-arginine methyl ester hydrochloride were not hydrolysed at the same enhanced level as casein. This is due primarily to the phosphorylated nature of casein. As it carries a net negative charge, the protein can interact with the positively charged amino terminals on the surface of GO through electrostatic interaction. Jin et al concluded that the amino terminals were the primary reason for trypsin bound to PEGylated-GOs showing enhanced reaction rate with phosphoproteins. Further to this kinetic studies revealed that at high concentrations casein can act as inhibitor of both free and bound trypsin, however the bound trypsin (GO PEGylated with 10k-6br-PEG-NH₂) accelerated the initial digestion of casein 43-fold higher than free trypsin. Trypsin's thermal stability at 70 and 80 °C was also improved when immobilised on the PEGylated GOs, demonstrating the contribution of GO in protecting the enzyme from denaturation.

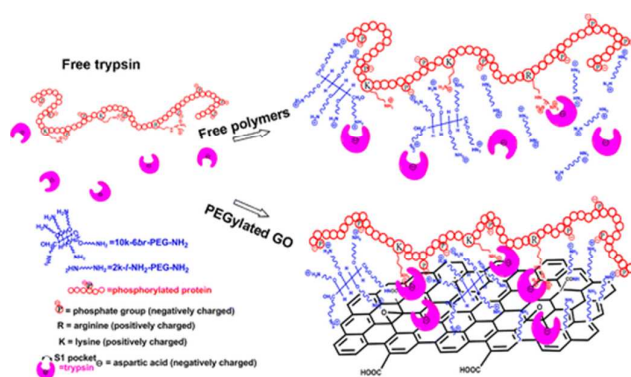


Fig. 13 Schematic representation of PEG-functionalised graphene oxide nanosheets with trypsin immobilised through electrostatic interactions, facilitating the cleavage of phosphorylated proteins. Reproduced with permission. Reprinted with permission from ref.⁸². Copyright 2012 American Chemical Society.

4.1.3 Concentration of enzymes

Owing to their large surface area and nano-scale size, 2D NMs can be loaded with exceptionally high amounts of enzyme relative to the mass of the support material. This allows for enzymes to be concentrated at a desired location, for instance in a bio-reactor. When used in enzyme reactors the concentration of enzymes in these immobilised materials can improve the reaction efficiency of the system.

Trypsin immobilised on unmodified GO in an immobilised enzyme reactor (IMER) appeared to work well for *in-situ* digestion of proteins.⁸⁰ Jiao et al immobilised trypsin on GO through electrostatic interaction and hydrogen bonding, using approximately 1mg.mg⁻¹ of the immobilised material for the digestion of proteins such as myoglobin, BSA and α -casein. Simultaneously, a control experiment with free trypsin was carried out. After 10 minutes of reaction, the digested products from both IMER and free trypsin were analysed using a MALDI-TOF mass spectrometer. The GO-IMER was able to release 30, 57 and 77% mass as peptides from BSA, α -casein and myoglobin, respectively. Whereas peptides from the digestion using free trypsin in solution were barely detectable in the given reaction time. This improved catalytic activity of trypsin bound to GO is largely due to the IMER, which was able to concentrate both the enzyme and protein substrates. While the bound enzyme may not be as active as the free trypsin, the increased loading capacity of GO allowed the binding of high concentrations of trypsin, increasing the digestion efficiency. The nano-scale of GO also allows for the miniaturisation of this technology.

Yin et al used a capillary electrophoresis-based IMER (CE-IMER) for the immobilisation of trypsin-GO complex for similar protein digestion and separation analysis to that of Jin et al.⁸¹ They used layer-by-layer assembly via electrostatic interaction to fabricate the immobilised trypsin into the reactor. The formed products were separated and monitored using spectrophotometric detection at 214 nm. It was found after immobilisation that the pH optima of immobilised trypsin shifted to 8.5 (pH 7.5 for free trypsin as determined by the authors) due to changes in the microenvironment in CE-IMER. However, the enzyme kinetic values ($K_m = 0.24 \pm 0.002$ mM, $V_{max} = 0.32 \pm 0.04$ mM.s⁻¹) remained close to that of free trypsin. This indicates that the method used to fabricate GO did not adversely alter the secondary structure of trypsin. Digestion of angiotensin and BSA in the CE-IMER was carried out between 3–30 min and the digested products were analysed using mass spectrometry. The results obtained were comparable to those obtained after a 12 h digestion with free trypsin in solution. In addition to GO, other 2D NMs such as MoS₂ and WSe₂ have also been used to bind high concentrations of enzymes and improve the catalytic properties of a system, in this case for biosensor applications.^{156, 158} These studies show that the microenvironment and the amount of enzyme loaded play important roles in controlling the catalytic properties enzyme systems.

4.1.4 Substrate channelling in bi-enzymatic systems

Research has begun on the use of bi-enzymatic systems on 2D NMs for sequential cascade reactions.^{68, 103} Bi-enzyme systems are appealing because they can potentially overcome the limitations of reactant transportation from one enzyme's catalytic site to that of another. This can reduce reaction with competing substrates and

prevent substrates from forming toxic intermediates.^{103, 159} Recently Mathesh et al developed a bi-enzymatic system for controlled substrate channelling from the catalytic site of GOx to HRP (Figure 15).⁶⁸ The advantage of surface hydrophobicity and the confined space between co-immobilised GOx and HRP, resulted in the amplifying of signal strength in the catalytic detection of glucose. This was improved 20-fold in comparison to that obtained with a free enzyme system.⁶⁸

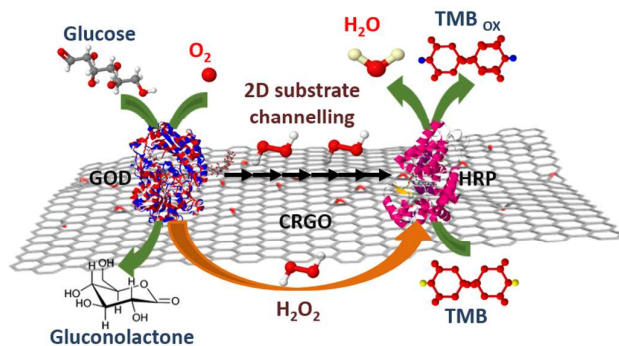


Fig. 15 Schematic representation for substrate channelling of H_2O_2 between glucose oxidase (GOx, referred to as GOD in this figure) and horseradish peroxidase (HRP). Reproduced from ref ⁶⁸ with permission from John Wiley and Sons.

Zhao et al immobilised glucoamylase (GA) in conjunction with GOx in order to demonstrate a one-pot reaction for the biocatalysis of starch to gluconic acid.¹⁰³ This was achieved by non-covalently binding the two enzymes onto CRGOs. The individual bound

enzymes were characterised with respect to temperature and pH as well as CRGO hydrophobicity. They found that both GOx and GA were most active on CRGO that was reduced for 2 h (by L-AA reduction), with GOx activity improved 2-fold compared to that of the free enzyme. This increase in activity was due to a combination of total enzyme loading (more enzyme was bound to more hydrophobic CRGOs) and improvement of enzyme activity, as more hydrophobic supports (CRGO 4 and 12 h) bound more protein but were less active. This suggests that while small changes to enzyme secondary structure caused by associations with weakly hydrophobic surfaces may be beneficial to activity, strongly hydrophobic surfaces likely deform the enzyme's structure and diminish activity. This is similar to observations made by Mathesh et al.¹¹⁵ Using the one-pot system Zhao et al were able to achieve a 72% conversion of starch to gluconic acid after three hours.¹⁰³ They could further control the rate of reaction by altering the amounts and ratio of both GOx and GA (as GOx catalysed the hydrolysis of starch at a higher rate than GA catalysed the formation of gluconic acid from glucose). When immobilising GA:GOx at a mass ratio of 1:1.3 in improved the conversion to 82% after 2 hours. It was also shown that the bi-enzymatic system bound to 2 h CRGO retained 85% of activity after four reaction cycles.

In the above, we have discussed examples from the literature where immobilisation of various enzymes on 2D NMs has led to modifications to their functional and/or structural properties. The examples discussed in Section 4 are summarised with respect to changes to enzyme activity, stability, selectivity and structure in Table 2.

Table 2. Summary of enzymes with properties modified by immobilisation on 2D NMs

Enzyme	2D NM	Immobilisation	Enzyme property reported to be modified				Ref
			Activity	Stability	Selectivity	Structure	
D-Psicose-3-epimerase	GO	Non-covalent	Temperature optima 50 ^b –60 °C Bioconversion of D-fructose to D-psicose increased 20 % ^a	Thermostability half-life improved 3.99 ^a –720 min	----	----	70
Horseradish peroxidase	GO	Non-covalent	Improved activity at basic pH ^a	36% activity retained at pH 10 (10% ^b); Thermostability after 120 min at 50 °C was 50% (<20% ^b) activity	Improved selectivity towards 2,4-dimethoxyphenol and 2-chlorophenol ^a	----	95
Trypsin	GO, PEGylated GO	Non-covalent	Casein hydrolysis increased 2-fold ^a on PEGylated GO	Thermostability shifted to 80 °C (40 ^b)	Improved for phosphorylated proteins ^a	----	82
Chymotrypsin	Graphene, GO	Non-covalent	----	----	----	S ₁ specific pocket deformation (MD simulation)	109

Journal Name							ARTICLE
Lysozyme	GO, rGO	Non-covalent	56.2% ^a activity on GO, 94.9% ^a activity on rGO	----	----	GO denatured Lysozyme (Trp fluorescence) Increased α -helix content (CD)	106
Lipase from <i>Alcaligenes</i> sp.	CRGOs	Non-covalent	pNPP hydrolysis increased 1.43-fold ^a on 4 h CRGO	60% activity retained after 60 days (enzyme paper)	----	α -helix/ β -sheet decreased (FTIR, CD); Lid opening (MD simulation)	115
Lipase from <i>Yarrowia lipolytica</i>	GO (COOH-functionalised)	Covalent	Olive oil hydrolysis 80% ^a ; (R,S)-1-phenylethanol 1.6 fold ^a increase in catalysis efficiency	----	Improved selectivity for (R)-1-phenylethanol ^a	23.6% α -helix decrease (CD) Lid opening (MD simulation)	112, 160
Lipase from <i>Rhizopus oryzae</i>	GO	Covalent and non-covalent	Non-covalent immobilisation decreased V_{max} for hydrolysis of pNPL by 15-19-fold ^a	Solvent stability improved in acetone (2.2-fold) and isopropanol (1.6-fold); Thermostability improved at 70 °C (6 ^b -65%)	Selectivity for esterification of longer-chain fatty acids	----	113, 114
Lipase B from <i>Candida antarctica</i>	GO (NH ₂ -functionalised)	Covalent Non-covalent	Esterification increased 1.3-fold ^a (covalent) and by 1.66-fold ^a (non-covalent)	Reaction cycling stability ~50% (non-covalent) and ~70% (covalent) activity after 7 cycles (168 h)	----	α -helix content increased 3% (covalent) and decreased 30% (non-covalent) (FTIR)	116
Glucose oxidase - Horseradish peroxidase (Co-immobilised)	CRGOs	Non-covalent	Sensitivity towards glucose increased 20-fold ^a	~85% activity after 2 months storage; reaction cycling stability ~70% activity after 6 cycles	----	Decrease in α -helix and increase in β -sheet (CD & FTIR)	68
Glucose oxidase Glucoamylase (Co-immobilised)	CRGOs	Non-covalent	GOx activity improved 2-fold ^a ; 82% conversion of starch to gluconic acid in 2 h	Thermostability after 2 hr at 50 °C retained 85% activity; reaction cycling stability 85% activity after 4 cycles	----	----	103

^a relative to the free enzyme; ^b value reported for free enzyme

5. Summary and perspectives

The interaction of graphene and other 2D NMs with biological molecules for a variety of bio-applications, such as biosensors, bio-fuel cells, drug delivery systems and tissue engineering, has increased dramatically in recent years. However, the use of 2D NMs for enzyme immobilisation, and controlling enzyme function for use as biocatalysts, is a relatively new area of research. The physical properties of 2D NMs enables interactions of enzymes with the materials to be investigated in solution, which is not possible with

traditional immobilisation supports. 2D NMs possess other unique properties, such as high surface areas and tunable surface chemistry, which make them highly versatile for biocatalytic applications. While there are numerous examples in the literature demonstrating the interaction of different biomolecules with 2D NMs for a range of bio-applications, this review focuses on recent approaches implemented for the immobilisation of enzymes. Furthermore, although the most common examples in the literature of enzymes being bound to 2D NMs are for biosensor fabrication,

this review focuses on the immobilisation strategies employed and their importance for biocatalysis.

A range of immobilisation strategies have been applied to bind enzymes to 2D NM surfaces to study and modify their catalytic properties. The concept of controlling enzyme activity, selectivity and stability by immobilisation on 2D NMs has been demonstrated by our group and others using biotechnologically important enzymes such as GOx, HRP, laccase and lipases. Factors such as surface charge density, hydrophobicity, surface functionalisation and cross-linking are important parameters for achieving effective enzyme immobilisation. While publications addressing some of these properties have been reviewed here, the field is in its infancy and there is still much to be investigated. Relatively few studies have investigated how specific surface properties of 2D NMs affect enzyme-support interactions and the effects that these have on catalysis. This is further complicated by active site topologies and conformations differing significantly between enzymes, and that their respective interactions with 2D NMs are as yet unpredictable. This variability between enzymes leads to difficulty in making generalisations about how surface properties will modify the activity of a specific enzyme. Enzyme immobilization is in many instances associated with a decrease in enzyme activity. Changes that lead to decreased activity are largely uncontrolled and this provides one of the greatest challenges; understanding how to tailor immobilisation for different enzymes, whether through support chemistry, immobilisation conditions or a combination of both, to achieve immobilisation in a controlled manner. Realising this, would yield biocatalysts with desired improvements with respect to activity, specificity, selectivity and stability. As further research in the area is published, new details will likely emerge that will enable a more targeted application of immobilisation to the modification of enzyme function. For this reason further studies with different enzyme classes are required.

Currently some key challenges are limiting the use of 2D NMs for large-scale biocatalytic applications. This includes control of material properties during synthesis and fabrication, particularly involving the dimensions of 2D NMs and their surface chemistry. In addition, concerns over their use in food-related processes present unknown risks with respect to toxicity and negative health effects. The application of these materials in large-scale biocatalysis, including food-grade applications, may preferably lie in the incorporation of 2D NMs into macrostructures. The synthesis of well-defined 'enzyme papers', 3D structures or composite materials with suitable flow properties for use in flow-through bio-reactors is a useful approach where the NMs are not free and hence are removable from the food material. Therefore as advanced chemistries are developed that can effectively control the properties of 2D NMs, we propose these challenges will be overcome. Despite the limitations to commercial-scale use (excluding biosensor fabrication), using 2D NMs for studying enzyme function remains a promising area of research and warrants further examination. Importantly, research performed now using 2D NMs as model systems to understand the effects of immobilisation on enzymes will aid in the development of future immobilisation supports and biocatalysts for industrial applications. We hope that many other researchers join this expanding area of research so that a comprehensive body of research can be

generated to further understand immobilisation mechanisms and how they impact enzyme structure and function.

Conflicts of interest

There are no conflicts to declare.

Acknowledgements

T. R. B. Ramakrishna gratefully acknowledges the PhD scholarship she has been provided with by Deakin University and Plant and Food Research New Zealand to undertake her studies. This work was partially supported by the New Zealand Ministry for Business, Innovation and Employment through the research programme 'Export Marine Products', contract number C11X1307; and the Australian Research Council LP140100722 and DP130101714.

References

1. K. S. Novoselov, A. K. Geim, S. V. Morozov, D. Jiang, Y. Zhang, S. V. Dubonos, I. V. Grigorieva and A. A. Firsov, *Science*, 2004, **306**, 666-669.
2. A. Peigney, C. Laurent, E. Flahaut, R. R. Bacsa and A. Rousset, *Carbon*, 2001, **39**, 507-514.
3. F. Bonaccorso, L. Colombo, G. Yu, M. Stoller, V. Tozzini, A. C. Ferrari, R. S. Ruoff and V. Pellegrini, *Science*, 2015, **347**.
4. L. Wang, W. Liu, Y. Zhang, Z.-H. Zhang, S. Tiam Tan, X. Yi, G. Wang, X. Sun, H. Zhu and H. Volkan Demir, *Nano Energy*, 2015, **12**, 419-436.
5. P. Blake, P. D. Brimicombe, R. R. Nair, T. J. Booth, D. Jiang, F. Schedin, L. A. Ponomarenko, S. V. Morozov, H. F. Gleeson, E. W. Hill, A. K. Geim and K. S. Novoselov, *Nano Lett.*, 2008, **8**, 1704-1708.
6. X. Huang, T. Leng, M. Zhu, X. Zhang, J. Chen, K. Chang, M. Aqeeli, A. K. Geim, K. S. Novoselov and Z. Hu, *Sci. Rep.*, 2015, **5**, 18298.
7. C. Lee, X. Wei, J. W. Kysar and J. Hone, *Science*, 2008, **321**, 385-388.
8. A. S. Mayorov, R. V. Gorbachev, S. V. Morozov, L. Britnell, R. Jalil, L. A. Ponomarenko, P. Blake, K. S. Novoselov, K. Watanabe, T. Taniguchi and A. K. Geim, *Nano Lett.*, 2011, **11**, 2396-2399.
9. A. A. Balandin, *Nat. Mater.*, 2011, **10**, 569-581.
10. R. Raccichini, A. Varzi, S. Passerini and B. Scrosati, *Nat. Mater.*, 2015, **14**, 271-279.
11. J. Zhu, D. Yang, Z. Yin, Q. Yan and H. Zhang, *Small*, 2014, **10**, 3480-3498.
12. D. A. C. Brownson, J. P. Metters and C. E. Banks, in *Nanotechnol. Energy Challenge*, Wiley-VCH Verlag GmbH & Co. KGaA, 2013, pp. 133-170.
13. Y. Wang, Z. Li, J. Wang, J. Li and Y. Lin, *Trends Biotechnol.*, 2011, **29**, 205-212.
14. Y. Zhang, T. R. Nayak, H. Hong and W. Cai, *Nanoscale*, 2012, **4**, 3833-3842.

15. E. Abbasi, A. Akbarzadeh, M. Kouhi and M. Milani, *Artif. Cells, Nanomed., Biotechnol.*, 2016, **44**, 150-156.
16. V. Nicolosi, M. Chhowalla, M. G. Kanatzidis, M. S. Strano and J. N. Coleman, *Science*, 2013, **340**.
17. C. Tan, X. Cao, X.-J. Wu, Q. He, J. Yang, X. Zhang, J. Chen, W. Zhao, S. Han, G.-H. Nam, M. Sindoro and H. Zhang, *Chem. Rev.*, 2017, **117**, 6225-6331.
18. H. Zhang, *ACS Nano*, 2015, **9**, 9451-9469.
19. O. Kirk, T. V. Borchert and C. C. Fuglsang, *Curr. Opin. Biotechnol.*, 2002, **13**, 345-351.
20. R. A. Sheldon and S. van Pelt, *Chem. Soc. Rev.*, 2013, **42**, 6223-6235.
21. U. Hanefeld, L. Cao and E. Magner, *Chem. Soc. Rev.*, 2013, **42**, 6211-6212.
22. U. Hanefeld, L. Gardossi and E. Magner, *Chem. Soc. Rev.*, 2009, **38**, 453-468.
23. S. Datta, L. R. Christena and Y. R. S. Rajaram, *3 Biotech*, 2013, **3**, 1-9.
24. R. C. Rodrigues, C. Ortiz, A. Berenguer-Murcia, R. Torres and R. Fernandez-Lafuente, *Chem. Soc. Rev.*, 2013, **42**, 6290-6307.
25. D. Chimene, D. L. Alge and A. K. Gaharwar, *Adv. Mater.*, 2015, **27**, 7261-7284.
26. D. Li, M. B. Müller, S. Gilje, R. B. Kaner and G. G. Wallace, *Nat. Nanotechnol.*, 2008, **3**, 101.
27. Y. Zhang, C. Wu, S. Guo and J. Zhang, *NTREV*, 2013, **2**, 27.
28. M. L. Verma, M. Puri and C. J. Barrow, *Crit. Rev. Biotechnol.*, 2016, **36**, 108-119.
29. V. C. Sanchez, A. Jachak, R. H. Hurt and A. B. Kane, *Chemical Research in Toxicology*, 2012, **25**, 15-34.
30. D. Li, W. Zhang, X. Yu, Z. Wang, Z. Su and G. Wei, *Nanoscale*, 2016, **8**, 19491-19509.
31. M. Zhang, Y. Li, Z. Su and G. Wei, *Polymer Chemistry*, 2015, **6**, 6107-6124.
32. K. Ariga, Q. Ji, T. Mori, M. Naito, Y. Yamauchi, H. Abe and J. P. Hill, *Chemical Society Reviews*, 2013, **42**, 6322-6345.
33. R. Ahmad and M. Sardar, *Biochem. and Anal. Biochem.*, 2015, **4**, 1.
34. S. C. Lau, H. N. Lim, M. Basri, H. R. Fard Masoumi, A. Ahmad Tajudin, N. M. Huang, A. Pandikumar, C. H. Chia and Y. Andou, *PLOS ONE*, 2014, **9**, e104695.
35. X. Zhou, M. Wang, J. Lian and Y. Lian, *Sci. China Technol. Sci.*, 2014, **57**, 278-283.
36. M. Mathesh, H. Wang, C. Barrow and W. Yang, *Journal*, 2015, 333-366.
37. J. Liu, Z. Liu, C. J. Barrow and W. Yang, *Anal. Chim. Acta*, 2015, **859**, 1-19.
38. K. S. Novoselov, D. Jiang, F. Schedin, T. J. Booth, V. V. Khotkevich, S. V. Morozov and A. K. Geim, *Proc. Natl. Acad. Sci. U. S. A.*, 2005, **102**, 10451-10453.
39. X. Li, W. Cai, J. An, S. Kim, J. Nah, D. Yang, R. Piner, A. Velamakanni, I. Jung, E. Tutuc, S. K. Banerjee, L. Colombo and R. S. Ruoff, *Science*, 2009, **324**, 1312-1314.
40. K. K. Kim, A. Hsu, X. Jia, S. M. Kim, Y. Shi, M. Hofmann, D. Nezich, J. F. Rodriguez-Nieva, M. Dresselhaus and T. Palacios, *Nano Lett.*, 2011, **12**, 161-166.
41. K. Novoselov and A. C. Neto, *Phys. Scr.*, 2012, **2012**, 014006.
42. S. Suzuki, Y. Takei, K. Furukawa and H. Hibino, *Appl. Phys. Express*, 2011, **4**, 065102.
43. J. Yang, Y. Gu, E. Lee, H. Lee, S. H. Park, M. H. Cho, Y. H. Kim, Y. H. Kim and H. Kim, *Nanoscale*, 2015, **7**, 9311-9319.
44. J. Zhang, H. Yang, G. Shen, P. Cheng, J. Zhang and S. Guo, *Chem. Comm.*, 2010, **46**, 1112-1114.
45. W. S. Hummers and R. E. Offeman, *J. Am. Chem. Soc.*, 1958, **80**, 1339-1339.
46. M. Lotya, Y. Hernandez, P. J. King, R. J. Smith, V. Nicolosi, L. S. Karlsson, F. M. Blighe, S. De, Z. Wang and I. McGovern, *J. Am. Chem. Soc.*, 2009, **131**, 3611-3620.
47. C.-J. Shih, A. Vijayaraghavan, R. Krishnan, R. Sharma, J.-H. Han, M.-H. Ham, Z. Jin, S. Lin, G. L. C. Paulus, N. F. Reuel, Q. H. Wang, D. Blankschtein and M. S. Strano, *Nat. Nanotechnol.*, 2011, **6**, 439.
48. G. Eda, H. Yamaguchi, D. Voiry, T. Fujita, M. Chen and M. Chhowalla, *Nano Lett.*, 2011, **11**, 5111-5116.
49. P. Joensen, R. F. Frindt and S. R. Morrison, *Mater. Res. Bull.*, 1986, **21**, 457-461.
50. Y. Hernandez, V. Nicolosi, M. Lotya, F. M. Blighe, Z. Sun, S. De, I. T. McGovern, B. Holland, M. Byrne, Y. K. Gun'Ko, J. J. Boland, P. Niraj, G. Duesberg, S. Krishnamurthy, R. Goodhue, J. Hutchison, V. Scardaci, A. C. Ferrari and J. N. Coleman, *Nat. Nanotechnol.*, 2008, **3**, 563.
51. J. N. Coleman, *Acc. Chem. Res.*, 2013, **46**, 14-22.
52. J. N. Coleman, M. Lotya, A. O'Neill, S. D. Bergin, P. J. King, U. Khan, K. Young, A. Gaucher, S. De, R. J. Smith, I. V. Shvets, S. K. Arora, G. Stanton, H.-Y. Kim, K. Lee, G. T. Kim, G. S. Duesberg, T. Hallam, J. J. Boland, J. J. Wang, J. F. Donegan, J. C. Grunlan, G. Moriarty, A. Shmeliov, R. J. Nicholls, J. M. Perkins, E. M. Grieveson, K. Theuvsissen, D. W. McComb, P. D. Nellist and V. Nicolosi, *Science*, 2011, **331**, 568-571.
53. C. Zhi, Y. Bando, C. Tang, H. Kuwahara and D. Golberg, *Adv. Mater.*, 2009, **21**, 2889-2893.
54. T. Tanaka, Y. Ebina, K. Takada, K. Kurashima and T. Sasaki, *Chem. Mater.*, 2003, **15**, 3564-3568.
55. R. Ma and T. Sasaki, *Adv. Mater.*, 2010, **22**, 5082-5104.

56. R. Ma, Z. Liu, L. Li, N. Iyi and T. Sasaki, *J. Mater. Chem.*, 2006, **16**, 3809-3813.
57. P. F. Luckham and S. Rossi, *Adv. Colloid Interface Sci.*, 1999, **82**, 43-92.
58. H. Zeng and X. Cui, *Chem. Soc. Rev.*, 2015, **44**, 2629-2642.
59. P. K. Chow, E. Singh, B. C. Viana, J. Gao, J. Luo, J. Li, Z. Lin, A. L. Elías, Y. Shi, Z. Wang, M. Terrones and N. Koratkar, *ACS Nano*, 2015, **9**, 3023-3031.
60. F. Taherian, V. Marcon, N. F. A. van der Vegt and F. Leroy, *Langmuir*, 2013, **29**, 1457-1465.
61. L. Staudenmaier, *Ber. Dtsch. Chem. Ges.*, 1898, **31**, 1481-1487.
62. B. C. Brodie, *Philos. Trans. R. Soc. London*, 1859, **149**, 249-259.
63. H.-P. Boehm and W. Scholz, *Justus Liebig's Ann. Chem.*, 1966, **691**, 1-8.
64. A. Lerf, H. He, M. Forster and J. Klinowski, *J. Phys. Chem. B*, 1998, **102**, 4477-4482.
65. A. Lerf, in *Graphene Oxide*, John Wiley & Sons, Ltd, 2016, pp. 1-35.
66. J. Wang, H. Zhu, Y. Xu, W. Yang, A. Liu, F. Shan, M. Cao and J. Liu, *Sens. Actuators, B*, 2015, **220**, 1186-1195.
67. Y. Zhang, J. Zhang, X. Huang, X. Zhou, H. Wu and S. Guo, *Small*, 2012, **8**, 154-159.
68. M. Mathesh, J. Liu, C. J. Barrow and W. Yang, *Chem. Eur. J*, 2017, **23**, 304-311.
69. R. C. Rodrigues, C. Ortiz, Á. Berenguer-Murcia, R. Torres and R. Fernández-Lafuente, *Chem. Soc. Rev.*, 2013, **42**, 6290-6307.
70. S. R. Dedania, M. J. Patel, D. M. Patel, R. C. Akhiani and D. H. Patel, *Enzyme Microb. Technol.*, 2017, **107**, 49-56.
71. L. Chen, B. Wei, X. Zhang and C. Li, *Small*, 2013, **9**, 2331-2340.
72. X. Wu, Y. Hu, J. Jin, N. Zhou, P. Wu, H. Zhang and C. Cai, *Anal. Chem.*, 2010, **82**, 3588-3596.
73. E. Skoronski, D. H. Souza, C. Ely, F. Broilo, M. Fernandes, A. Fúrigo and M. G. Ghislandi, *Int. J. Biol. Macromol.*, 2017, **99**, 121-127.
74. M. Patila, A. Kouloumpis, D. Gournis, P. Rudolf and H. Stamatis, *Sensors (Basel)*, 2016, **16**, 287.
75. S. K. S. Patel, S. H. Choi, Y. C. Kang and J.-K. Lee, *ACS Appl. Mater. Interfaces*, 2017, **9**, 2213-2222.
76. H. Li, J. Hou, L. Duan, C. Ji, Y. Zhang and V. Chen, *J. Hazard. Mater.*, 2017, **338**, 93-101.
77. F. Qu, X. Ma, Y. Hui, F. Chen and Y. Gao, *Chin. J. Chem.*, 2017, **35**, 1098-1108.
78. Y. Song, C. Chen and C. Wang, *Nanoscale*, 2015, **7**, 7084-7090.
79. T. M. B. F. Oliveira, M. F. Barroso, S. Morais, M. Araújo, C. Freire, P. de Lima-Neto, A. N. Correia, M. B. P. P. Oliveira and C. Delerue-Matos, *Bioelectrochemistry*, 2014, **98**, 20-29.
80. J. Jiao, A. Miao, X. Zhang, Y. Cai, Y. Lu, Y. Zhang and H. Lu, *Analyst*, 2013, **138**, 1645-1648.
81. Z. Yin, W. Zhao, M. Tian, Q. Zhang, L. Guo and L. Yang, *Analyst*, 2014, **139**, 1973-1979.
82. L. Jin, K. Yang, K. Yao, S. Zhang, H. Tao, S.-T. Lee, Z. Liu and R. Peng, *ACS Nano*, 2012, **6**, 4864-4875.
83. D. Kishore, M. Talat, O. N. Srivastava and A. M. Kayastha, *PLoS One*, 2012, **7**, e40708.
84. W. Zhuang, L. He, J. Zhu, J. Zheng, X. Liu, Y. Dong, J. Wu, J. Zhou, Y. Chen and H. Ying, *Colloids Surf., B*, 2016, **145**, 785-794.
85. X. Ren, H. Bai, Y. Pan, W. Tong, P. Qin, H. Yan, S. Deng, R. Zhong, W. Qin and X. Qian, *Anal. Methods*, 2014, **6**, 2518-2525.
86. D. Wang, W. Dou, Y. Chen and G. Zhao, *RSC Adv.*, 2014, **4**, 57733-57742.
87. L.-M. Lu, X.-L. Qiu, X.-B. Zhang, G.-L. Shen, W. Tan and R.-Q. Yu, *Biosens. Bioelectron.*, 2013, **45**, 102-107.
88. S. Nalini, S. Nandini, S. Shanmugam, S. E. Neelagund, J. S. Melo and G. S. Suresh, *J. Solid State Electrochem.*, 2014, **18**, 685-701.
89. A. Pattammattel, M. Puglia, S. Chakraborty, I. K. Deshapriya, P. K. Dutta and C. V. Kumar, *Langmuir*, 2013, **29**, 15643-15654.
90. C. Zhang, S. Chen, P. J. J. Alvarez and W. Chen, *Carbon*, 2015, **94**, 531-538.
91. J. Liu, T. Wang, J. Wang and E. Wang, *Electrochim. Acta*, 2015, **161**, 17-22.
92. Q. Zeng, J. Cheng, L. Tang, X. Liu, Y. Liu, J. Li and J. Jiang, *Adv. Funct. Mater.*, 2010, **20**, 3366-3372.
93. A. Muthurasu and V. Ganesh, *Appl. Biochem. Biotechnol.*, 2014, **174**, 945-959.
94. G. Lai, H. Cheng, D. Xin, H. Zhang and A. Yu, *Anal. Chim. Acta*, 2016, **902**, 189-195.
95. F. Zhang, B. Zheng, J. Zhang, X. Huang, H. Liu, S. Guo and J. Zhang, *J. Phys. Chem. C*, 2010, **114**, 8469-8473.
96. J. Zhang, F. Zhang, H. Yang, X. Huang, H. Liu, J. Zhang and S. Guo, *Langmuir*, 2010, **26**, 6083-6085.
97. Q. Sheng, M. Wang and J. Zheng, *Sens. Actuators, B*, 2011, **160**, 1070-1077.
98. Y. Liu, Q. Li, Y.-Y. Feng, G.-S. Ji, T.-C. Li, J. Tu and X.-D. Gu, *Chem. Pap.*, 2014, **68**, 732-738.
99. G. Srivastava, K. Singh, M. Talat, O. N. Srivastava and A. M. Kayastha, *PLOS ONE*, 2014, **9**, e113408.
100. N. Liu, G. Liang, X. Dong, X. Qi, J. Kim and Y. Piao, *Chem. Eng. J.*, 2016, **306**, 1026-1034.
101. L. Baptista-Pires, B. Pérez-López, C. C. Mayorga-Martinez, E. Morales-Narváez, N. Domingo, M. J. Esplandiu, F. Alzina, C. M. S. Torres and A. Merkoçi, *Biosens. Bioelectron.*, 2014, **61**, 655-662.

102. M. Amirbandeh and A. Taheri-Kafrani, *Int. J. Biol. Macromol.*, 2016, **93**, 1183-1191.
103. F. Zhao, H. Li, Y. Jiang, X. Wang and X. Mu, *Green Chem.*, 2014, **16**, 2558-2565.
104. N. Dutta, S. Biswas and M. K. Saha, *Enzyme Microb. Technol.*, 2016, **95**, 248-258.
105. N. Dutta, D. Raj, N. Biswas, M. Mallick and S. Omesh, *Biocatal. Agric. Biotechnol.*, 2017, **9**, 240-247.
106. Y. Bai, Z. Ming, Y. Cao, S. Feng, H. Yang, L. Chen and S.-T. Yang, *Colloids Surf., B*, 2017, **154**, 96-103.
107. M. De, S. S. Chou and V. P. Dravid, *J. Am. Chem. Soc.*, 2011, **133**, 17524-17527.
108. C. Sun, K. L. Walker, D. L. Wakefield and W. R. Dichtel, *Chem. Mater.*, 2015, **27**, 4499-4504.
109. X. Sun, Z. Feng, T. Hou and Y. Li, *ACS Appl. Mater. Interfaces*, 2014, **6**, 7153-7163.
110. X. Yang, C. Zhao, E. Ju, J. Ren and X. Qu, *Chem. Comm.*, 2013, **49**, 8611-8613.
111. L. Zuccaro, C. Tesauro, T. Kurkina, P. Fiorani, H. K. Yu, B. R. Knudsen, K. Kern, A. Desideri and K. Balasubramanian, *ACS Nano*, 2015, **9**, 11166-11176.
112. Q. Li, F. Fan, Y. Wang, W. Feng and P. Ji, *Ind. Eng. Chem. Res.*, 2013, **52**, 6343-6348.
113. S. Hermanová, M. Zarevúcká, D. Bouša, M. Pumera and Z. Sofer, *Nanoscale*, 2015, **7**, 5852-5858.
114. S. Hermanová, M. Zarevúcká, D. Bouša, M. Mikulics and Z. Sofer, *Appl. Mater. Today*, 2016, **5**, 200-208.
115. M. Mathesh, B. Luan, T. O. Akanbi, J. K. Weber, J. Liu, C. J. Barrow, R. Zhou and W. Yang, *ACS Catal.*, 2016, **6**, 4760-4768.
116. I. V. Pavlidis, T. Vorhaben, T. Tsoufis, P. Rudolf, U. T. Bornscheuer, D. Gournis and H. Stamatis, *Bioresour. Technol.*, 2012, **115**, 164-171.
117. T. Wang, J. Liu, J. Ren, J. Wang and E. Wang, *Talanta*, 2015, **143**, 438-441.
118. Y. Zhang, C. Wu, J. Zhang and S. Guo, *J. Electrochem. Soc.*, 2017, **164**, B29-B33.
119. V. Sethuraman, P. Muthuraja, J. Anandha Raj and P. Manisankar, *Biosens. Bioelectron.*, 2016, **84**, 112-119.
120. A. Gong, C.-T. Zhu, Y. Xu, F.-Q. Wang, D. a. K. Tsabing, F.-A. Wu and J. Wang, *Sci. Rep.*, 2017, **7**, 4309.
121. E. Piccinini, C. Bliem, C. Reiner-Rozman, F. Battaglini, O. Azzaroni and W. Knoll, *Biosens. Bioelectron.*, 2017, **92**, 661-667.
122. T. Liu, H. Su, X. Qu, P. Ju, L. Cui and S. Ai, *Sens. Actuators, B*, 2011, **160**, 1255-1261.
123. N. ZHOU, C. LI, R. MO, P. ZHANG, L. HE, F. NIE, W. SU, S. LIU, J. GAO, H. SHAO, Z.-J. QIAN and H. Ji, *Surf. Rev. Lett.*, 2016, **23**, 1550103.
124. K.-J. Huang, D.-J. Niu, X. Liu, Z.-W. Wu, Y. Fan, Y.-F. Chang and Y.-Y. Wu, *Electrochim. Acta*, 2011, **56**, 2947-2953.
125. U. Ghoshdastider, R. Wu, B. Trzaskowski, K. Mlynarczyk, P. Miszta, M. Gurusaran, S. Viswanathan, V. Renugopalakrishnan and S. Filipek, *RSC Adv.*, 2015, **5**, 13570-13578.
126. J. Guo, T. Zhang, C. Hu and L. Fu, *Nanoscale*, 2015, **7**, 1290-1295.
127. G. Zeng, Y. Xing, J. Gao, Z. Wang and X. Zhang, *Langmuir*, 2010, **26**, 15022-15026.
128. E. Mehmeti, D. M. Stanković, S. Chaiyo, J. Zavasnik, K. Žagar and K. Kalcher, *Microchim. Acta*, 2017, **184**, 1127-1134.
129. S. Alwarappan, C. Liu, A. Kumar and C.-Z. Li, *J. Phys. Chem. C*, 2010, **114**, 12920-12924.
130. C. Liu, Z. Chen and C. Z. Li, *IEEE Trans. Nanotechnol.*, 2011, **10**, 59-62.
131. C. Ruan, W. Shi, H. Jiang, Y. Sun, X. Liu, X. Zhang, Z. Sun, L. Dai and D. Ge, *Sensors and Actuators B: Chemical*, 2013, **177**, 826-832.
132. J. Liu, N. Kong, A. Li, X. Luo, L. Cui, R. Wang and S. Feng, *Analyst*, 2013, **138**, 2567-2575.
133. M. Zhang, C. Liao, C. H. Mak, P. You, C. L. Mak and F. Yan, *Sci. Rep.*, 2015, **5**, 8311.
134. M. V. A. Martins, A. R. Pereira, R. A. S. Luz, R. M. Iost and F. N. Crespilho, *Phys. Chem. Chem. Phys.*, 2014, **16**, 17426-17436.
135. M. M. Barsan, M. David, M. Florescu, L. Ţugulea and C. M. A. Brett, *Bioelectrochemistry*, 2014, **99**, 46-52.
136. B. Liang, X. Guo, L. Fang, Y. Hu, G. Yang, Q. Zhu, J. Wei and X. Ye, *Electrochem. Commun.*, 2015, **50**, 1-5.
137. D. Das, S. Ghosh and I. Basumallick, *Electroanalysis*, 2014, **26**, 2408-2418.
138. M. J. Novak, A. Pattammattel, B. Koshmerl, M. Puglia, C. Williams and C. V. Kumar, *ACS Catal.*, 2016, **6**, 339-347.
139. Y.-Q. Zhang, Y.-J. Fan, L. Cheng, L.-L. Fan, Z.-Y. Wang, J.-P. Zhong, L.-N. Wu, X.-C. Shen and Z.-J. Shi, *Electrochim. Acta*, 2013, **104**, 178-184.
140. X. Wang and X. Zhang, *Electrochim. Acta*, 2013, **112**, 774-782.
141. J. Yang, S. Deng, J. Lei, H. Ju and S. Gunasekaran, *Biosens. Bioelectron.*, 2011, **29**, 159-166.
142. Y. Jiang, Q. Zhang, F. Li and L. Niu, *Sens. Actuators, B*, 2012, **161**, 728-733.
143. J.-D. Qiu, J. Huang and R.-P. Liang, *Sens. Actuators, B*, 2011, **160**, 287-294.
144. T. T. Baby, S. S. J. Aravind, T. Arockiadoss, R. B. Rakhi and S. Ramaprabhu, *Sens. Actuators, B*, 2010, **145**, 71-77.
145. Y. Liu, D. Yu, C. Zeng, Z. Miao and L. Dai, *Langmuir*, 2010, **26**, 6158-6160.

146. P. Wu, Q. Shao, Y. Hu, J. Jin, Y. Yin, H. Zhang and C. Cai, *Electrochim. Acta*, 2010, **55**, 8606-8614.
147. H. Wu, J. Wang, X. Kang, C. Wang, D. Wang, J. Liu, I. A. Aksay and Y. Lin, *Talanta*, 2009, **80**, 403-406.
148. Z. Wang, X. Zhou, J. Zhang, F. Boey and H. Zhang, *J. Phys. Chem. C*, 2009, **113**, 14071-14075.
149. C. Shan, H. Yang, J. Song, D. Han, A. Ivaska and L. Niu, *AnalChem*, 2009, **81**, 2378-2382.
150. X. Kang, J. Wang, H. Wu, I. A. Aksay, J. Liu and Y. Lin, *Biosens. Bioelectron.*, 2009, **25**, 901-905.
151. S. Palanisamy, S. Cheemalapati and S.-M. Chen, *Mater. Sci. Eng. C.*, 2014, **34**, 207-213.
152. N. Haghighi, R. Hallaj and A. Salimi, *Mater. Sci. Eng. C.*, 2017, **73**, 417-424.
153. C. Wu, S. Yu and S. Lin, *Express Polym. Lett.*, 2014, **8**.
154. H. Chung, M. J. Kim, K. Ko, J. H. Kim, H.-a. Kwon, I. Hong, N. Park, S.-W. Lee and W. Kim, *Sci. Total Environ.*, 2015, **514**, 307-313.
155. J. Li, L.-J. Wu, S.-S. Guo, H.-E. Fu, G.-N. Chen and H.-H. Yang, *Nanoscale*, 2013, **5**, 619-623.
156. S. Su, H. Sun, F. Xu, L. Yuwen, C. Fan and L. Wang, *Microchim. Acta*, 2014, **181**, 1497-1503.
157. K. Zhou, Y. Zhu, X. Yang, J. Luo, C. Li and S. Luan, *Electrochim. Acta*, 2010, **55**, 3055-3060.
158. M. Z. M. Nasir, C. C. Mayorga-Martinez, Z. Sofer and M. Pumera, *ACS Nano*, 2017, **11**, 5774-5784.
159. L. Li, B. Liang, F. Li, J. Shi, M. Mascini, Q. Lang and A. Liu, *Biosens. Bioelectron.*, 2013, **42**, 156-162.
160. W. Feng, X. Sun and P. Ji, *Soft Matter*, 2012, **8**, 7143-7150.